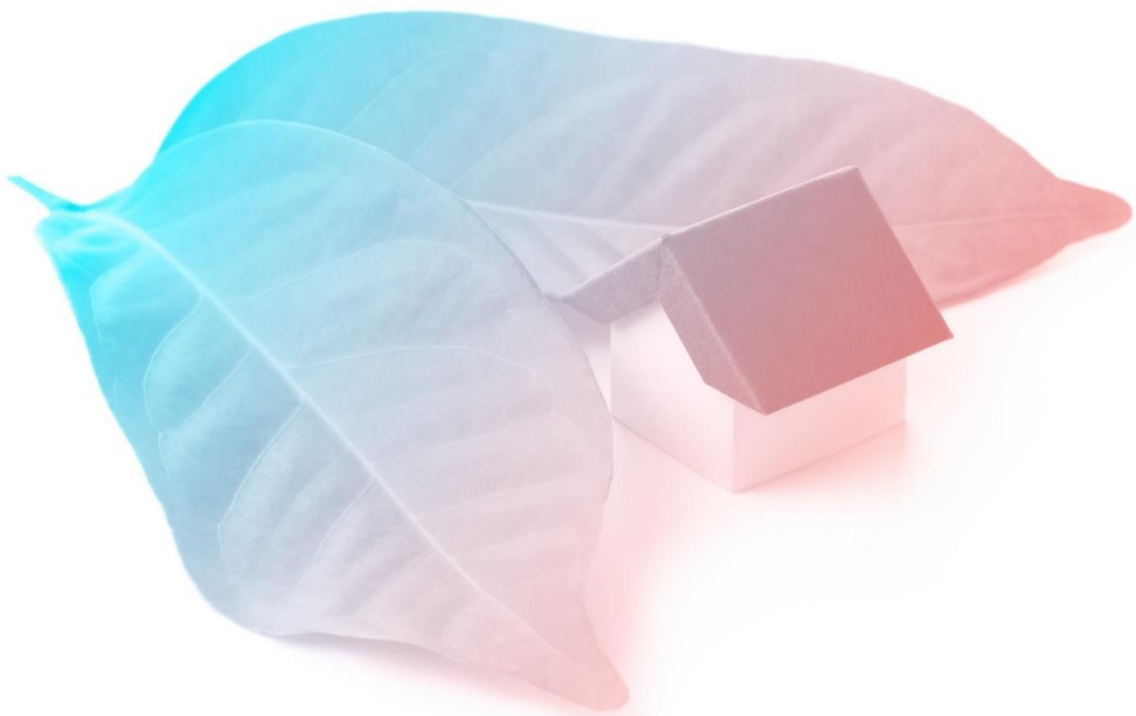




D4.1 Numerical optimisation of the reactive salt compound and vessel (Design of the TCM reactor)



Authors CNRS – PROMES : Driss Stitou
Maxime Perier-Muzet
Moad Mahboub
Roger Garcia



This project has received funding from the European Union's Horizon 2020 research and innovation programme under the grant agreement No 869821

D4.1 Numerical optimisation of the reactive salt compound and vessel (Design of the TCM reactor)

Summary			
<p>Deliverable D4.1 provides information and specifications for the TCM reactive material to be implemented in the Ministor thermochemical (TCM) reactor and the design of the thermochemical reactor that must be integrated in the TCM storage unit exploiting the low temperature thermal energy delivered by PVTs or FPCs collectors. The whole TCM storage process must ensure the dual function of storing the thermal energy from the solar collectors and its restitution in the form of cold during the summer or heat during winter. The first step in the development of such a system is the choice of the reactive salt capable of reacting with ammonia, the refrigerant, to meet the operating conditions of the Ministor system during the heating mode in winter and the cooling mode in summer. Ammonia (NH₃) was chosen as the refrigerant fluid since it has an interesting energy density while being stable over the temperature range considered for the Ministor application. Furthermore, it meets the requirements for the development of an environmental friendly system. Calcium chloride (CaCl₂) was selected over barium chloride (BaCl₂) as the reactive salt using thermodynamic calculations which allow to determine the equilibrium temperatures and pressures of the reaction with ammonia. Its implementation allows suitable heat and mass transfer properties, which are strongly correlated to the thermal power and energy density of the system. Enhancements to the salt are also considered such as addition of graphite.</p> <p>A simplified steady-state model describing a compressor-assisted transformation of the TCM reactor during the charging phase has been developed in order to carry out the design of a TCM unit according to : the targeted energy storage of the reactive medium (TCM energy density of 200 kWh/m³ fixed in the proposal), the required storage capacity and thermal powers in accordance with thermal needs or solar energy resources, the operating conditions such as solar resource available (power, temperature, duration) and the characteristics of the selected ammonia compressor.</p>			
Deliverable Number		Work Package	
D4.1		WP4	
Lead Beneficiary		Deliverable Author(S)	
CNRS PROMES		Driss Stitou Moad Mahboub, Maxime Perier Muzet, Roger Garcia	
Beneficiaries		Deliverable Co-Author (S)	
Beneficiaries		Deliverable Reviewer (S)	
TYNDALL-IERC		Carlos Ochoa, Maria Lopez Rosemarie MacSweeney	
Planned Delivery Date		Actual Delivery Date	
31/1/2021		03/11/2021 Revised version	
Type of deliverable	R	Report	X
Dissemination Level	CO	Confidential, only for members of the consortium (including the Commission)	
	PU	Public	X

Index

Index

Index	3
List of Tables	4
List of Figures	5
1. Scope, objective and structure of the deliverable	8
2. Choice of the reactive salts per operating conditions	11
3. TCM system configurations using a thermochemical reactor implementing either BaCl₂ or CaCl₂ salt.	15
4. Implementation characteristics of the TCM reactive material	20
4.1 Characteristics of the ENG/Salt composite TCM material	22
4.2 Heat transfer and mass transfer characteristics of the TCM reactive material	25
4.3 Final characteristics choice of the TCM material	28
5. Design of the TCM reactor	31
5.1 Model development for TCM reactor design	31
5.2 Design parametric study	33
5.3 Modular design and dimensioning of the TCM reactor	35
6. Conclusions	42
7. References	43

List of Tables

Table 1 Energy density and cost of the stored energy for the selected salts	13
Table 2 Characteristics of ammoniated calcium chloride salts and corresponding reaction	19
Table 3 TCM material characteristics.....	28
Table 4 Characteristics of two different design TCM storage unit for two heat storage capacity, 30 kWh with 13 reactor tubes or 16.3 kWh with 7 reactor tubes respecting the constraint of 200 kWh/m ³ of TCM material.....	37
Table 5 Operating parameters of the TCM storage for winter and summer conditions	39



List of Figures

Figure 1: Schematic description of the different operating phases of a basic solid-gas thermochemical sorption system. 9
Figure 2 Schema of TCM storage unit implemented in the Ministor system 9
Figure 3: Equilibrium curves of some ammoniated salts that can be considered for low temperature storage application such as Ministor storage.13
Figure 4: (P-T) diagram of the reaction equilibria that can be considered for Ministor $\text{BaCl}_2 \cdot (8/0)\text{NH}_3$, $\text{CaCl}_2 \cdot (8/4)\text{NH}_3$, $\text{CaCl}_2 \cdot (4/2)\text{NH}_3$ for TCM unit, and NH_3 phase-change.14
Figure 5: Thermodynamic operating conditions of TCM storage in storage mode in winter.15
Figure 6 : Thermodynamic operating conditions of TCM storage in discharge mode in winter.16
Figure 7: Thermodynamic operating conditions of TCM storage in discharge mode in summer.17
Figure 8: Thermodynamic operating conditions of TCM storage in discharge mode in summer.18
Figure 9: Raw materials used for the TCM reactive composite.20
Figure 10: Natural graphite flakes, Intercalated graphite flakes and Expanded ENG worm.21
Figure 11: $\text{CaCl}_2/\text{H}_2\text{O}$ phase diagram.21
Figure 12: Schematic view of the salt/ENG composite.22
Figure 13: Maximum energy density of the TCM material considering either the 1 st reaction or the 1 st and 2 nd reaction, as a function of the salt mass ratio and apparent bulk density of ENG in the TCM material.24
Figure 14: Evolution of the porosity of the TCM composite material when fully charged with ammonia ($\text{CaCl}_2 \cdot 8\text{NH}_3$), as a function of the apparent ENG density and salt mass ratio.25
Figure 15: Evolution of permeability of the fully charged TCM material with the anhydrous salt mass ratio and the apparent bulk density of ENG.27
Figure 16: Evolution of NH_3 permeability of the TCM material when fully charged with $\text{CaCl}_2 \cdot 8\text{NH}_3$ as function of the porosity and anhydrous salt mass ratio.27
Figure 17: Evolution of the thermal conductivity and NH_3 permeability of the fully charge TCM material reactive material ($\text{CaCl}_2 \cdot 8\text{NH}_3$)/ENG containing 85% an anhydrous salt, as a function of the apparent density of ENG in the reactive material.28
Figure 18: Evolution the bulk density of the TCM material as a function of the apparent ENG density and the salt mass ratio.28
Figure 19 : Evolution of the storage energy density of the TCM material and the TCM unit storage capacity of as a function of the advancement ΔX_2 of the second reaction considering an advancement of $\Delta X_1=0.95$ for the first reaction29
Figure 20: Required total length of reactor tube (4"OD) as a function of heat storage capacity of the TCM unit for an energy density of 200 kWh/m ³31
Figure 21: Evolution of the mass of cycled ammonia (red line) and the corresponding TCM reactive material mass (blue line) to be implemented considering advancements of reaction of reaction $\Delta X_1=0.95$ and $\Delta X_2=0.32$ to reach an energy density of 200 kWh/m ³ for a given heat storage capacity of the TCM reactor. Evolution of the corresponding maximum mass of ammonia that could be cycled if the second reaction is almost completed ($\Delta X_2=0.95$).31

Figure 22: Schematics of the TCM unit components and the different operating variables used for the modelling of the compressor driven TCM storage during the charging phase. Top left: View of an already shell and tube type reactor experimented in CNRS lab. Top right: View of the foreseen ammonia semi-hermetic compressor (Frigopol)32
Figure 23: FRIGOPOL semi-hermetic compressor model34
Figure 24: Evolution of the heat storage capacity of a shell and tube type TCM reactor as a function of the charging duration (i.e.:solar energy collected over a given time), the maximum swept volume of ammonia compressor Frigopol models (winter conditions for inlet PVT temperature = 60°C).34
Figure 25: Evolution of the required thermal heating power for of a shell and tube type TCM reactor, as a function of the charging duration (i.e.:solar energy collected over a given time), the maximum swept volume of ammonia compressor Frigopol models (winter conditions for inlet PVT temperature = 60°C).35
Figure 26: Evolution of the electrical consumption of the compressor and the volumetric ammonia flow rate pumped from the reactor as function of charging phase duration.35
Figure 27: Simulated results of a shell and tube type TCM reactor with different storage capacities coupled to a NH ₃ compressor with different given swept volumes (from 7.22 m ³ /h to 19.47 m ³ /h - Frigopol DLY models) - Required charging durations in winter (blue lines) and in summer (red lines) as a function of the inlet PVT thermal fluid temperature.36
Figure 28: TCM reactor tubes characteristics and proposed shell/tube design of the TCM reactor.37
Figure 29: TCM design solution for more energy flexibility and evolution of the TCM storage capacity for a given connected reactor tubes.40
Figure 30 : Volumetric flow of the Solar heat transfer fluid as a function of the thermal power.41
Figure 31: Evolution of the operating duration for a full charging of the 30kWh TCM reactor as a function of the thermal power provided by the solar field.41
Figure 32: Evolution of the wall temperature of the 30kWh TCM reactor as a function of the solar thermal power provided at 60°C.41
Figure 33: Evolution of the operating pressure of the TCM reactor as a function of the solar thermal power provided at 60°C.42
Figure 34: Evolution of the electrical consumption of the TCM reactor as a function of the solar thermal power provided at 60°C.42
Figure 35: Evolution of the swept volume to be applied to the Frigopol 7DLY compressor model.42
Figure 36: Evolution of the condenser thermal power operating at 28°C.43

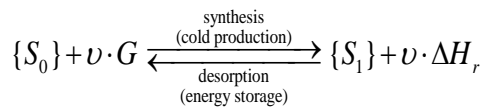
List of Abbreviations and Acronyms

Abbreviation	Definition
EU	European Union
G	Reactive gas (ammonia)
De	Energy density (kWh/m ³ of composite)
ENG	Expanded Natural Graphite
k	Permeability (m ²)
hsw	Thermal conductance between the wall of the reactor and the TCM material (W/m ² .K)
HEX	Heat exchanger
HP	Heat Pump
HTF	Heat transfer fluid
\dot{m}	Mass flow rate of the heat transfer fluid (kg/s)
M, Mm	Mass (kg) or Molar mass (kg/mole)
P	Pressure (Bar)
PCM	Phase Change Material
PV	Photovoltaic
PVT	Photovoltaic-thermal collector
R	Perfect gas constant (J/mol•K)
RES	Renewable Energy Sources
Q_{swept}	Swept volumetric flow rate of the NH ³ compressor (m ³ /s)
Q_v	Volumetric flow rate (m ³ /s)
So	Reactive salt with low content of reactive gas G
S1	Reactive salt with high content of reactive gas G
T	Temperature (°C)
TCM	ThermoCheMical
U	Overall heat transfer coefficient (W/m ² K)
V	Volume (m ³)
Vm	Molar volume (m ³ /mole)
X	Salt conversion ratio (moles of charged salt/ total moles of salt)
ΔH	Enthalpy of reaction or phase change (J/mol)
ΔS	Entropy of reaction or phase change (J/mol•K)
ΔX	Advancement rate of the reaction
$\rho_{\text{ENG}}, \rho_{\text{COMP}}$	Apparent density of the graphite, Bulk density of the TCM material (kg/m ³)
τ_s	Salt mass ratio (kg anhydrous salt/kg composite)
v	Stoichiometric coefficient of the reaction
ε	Porosity of the material (-)
λ	Thermal conductivity of the material (W/mK)

1. Scope, objective and structure of the deliverable

The scope of deliverable D4.1 is the determination of the best suitable reactive material that must be implemented into the thermochemical storage unit and to optimize the design of a compact thermochemical storage that meets the requirements of the Ministor project, the main objective of which is to provide a clean energy solution to meet the EU's long term energy strategy [1].

The principle of solid/gas (S/G) thermochemical sorption processes is based on the thermal effect of a reversible reaction between a solid (S) and a reactive gas (G). The strong chemical bonding involved in these reactions translates into high values of heat of reaction ΔH_r , and important amount of thermal energy can be stored in the salt into chemical form. The reaction follows the general equation: The strong chemical bonding involved in these reactions translates into and high thermal energy amount that can be stored in the salt into chemical form



where S_1 is salt rich in gas, S_0 is salt poor in gas, ν is the stoichiometric coefficient and ΔH_r is the enthalpy of the reaction per mole of gas. In order to implement a basic TCM storage unit the above solid/gas reaction from is coupled with a liquid/gas phase change process of the same working gas:



A thermochemical storage system that is based on such reversible reactions needs thus three components for its most basic implementation: a solid/gas reactor that contains the salt, which is alternatively connected to a condenser during the charging phase and the evaporator during the discharging phase.

From right to left, the reaction is called desorption. In this phase, thermal energy is transformed into chemical potential for a delayed useful energy production. The solid S_1 , charged with gas, absorbs an amount of heat (i.e., endothermic process), releases the gas and transforms into S_0 . The gas flows out of the reactor to the condenser, where it condensates and continues to the reservoir, where it is stored in liquid form.

From left to right, the reaction is called synthesis and it carried in the discharge mode for a useful heat /or cold production. The solid S_0 absorbs and reacts in an exothermic manner with the gas coming from the evaporator, forming the salt S_1 and producing the heat of reaction that can be used for heating purpose of the building in winter or released to the environment in summer. The basic process has thus two distinct phases an energy storage phase and a heat or cold production phase, which are related to the direction of the considered reaction. Figure 1 shows such an implementation in its simplest form. Such a process has been successfully tested for solar air conditioning, seasonal storage and various applications [1-10].

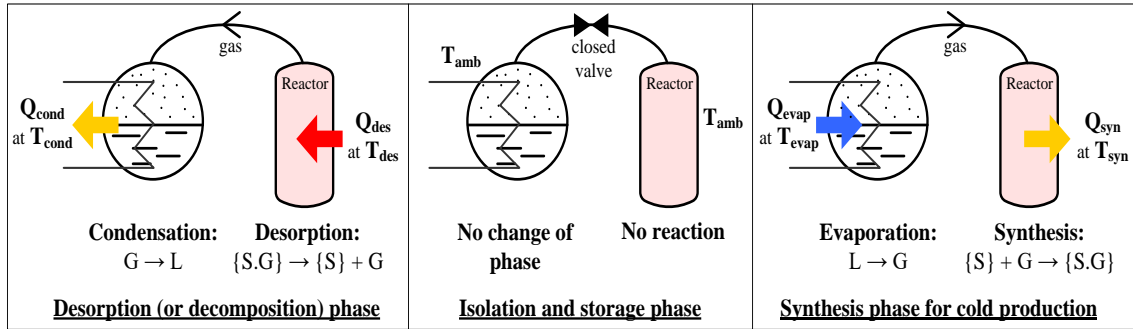


Fig. 1. Schematic description of the different operating phases of a basic solid-gas thermochemical sorption system.

In Ministor project, the heat of condensation is upgraded and valorised throughout a conventional heat-pump. Furthermore, an ammonia compressor is implemented to adapt the operating conditions of the reactor during the charging phase to the low grade heat provided at relatively low temperature by the PVT collectors. The use of a compressor installed between the condenser and the reactor, during the storage phase enables to lower the temperature of the heat source needed for the decomposition of the salt. The compressor forces the gas to flow from the reactor toward the condenser, even when the reactor pressure is lower than the condensing pressure. In this way, desorption temperature can be lowered, making it possible to upgrade and valorize of a wide range of low-temperature heat sources, such as those delivered by solar PVTs. The compressor therefore adapts the operating of the TCM reactor according to the heat source temperature independently to the operations conditions of the condenser. Figure 1 shows the foreseen implementation of such thermochemical storage in the Ministor system.

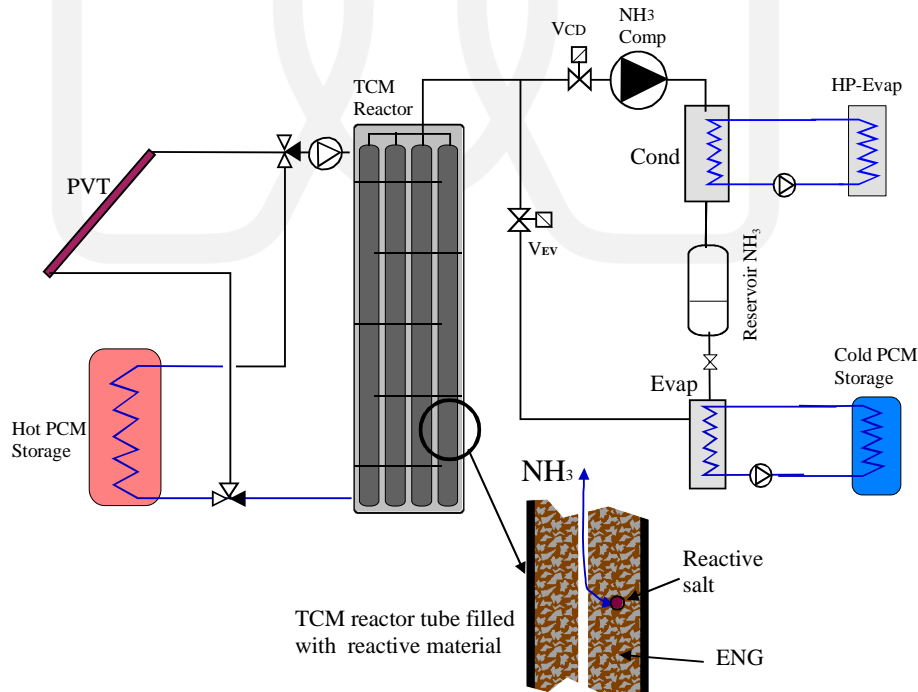


Figure 2 : Schema of TCM storage unit implemented in the Ministor system

The choice of the reactive must meet the different operating conditions that are imposed to the TCM unit during winter and summer. The thermal power and energy density of the TCM reactor are strongly impacted by the quality of heat and mass transfers taking place in such solid/gas reactors. The mixing of

the reactive salt with a thermal and consolidating binder, such as the Expanded Natural Graphite (ENG), enables to enhance the thermal conductivity and gas permeability of reactive material placed in fixed bed thermochemical reactor [11-13]. This implementation of the reactant salt with ENG is simply made by physically mixing the two compounds and compressing them in a mould or directly in the reactor tube. The obtained ENG/salt composite is sufficiently consolidated to be manipulated and homogeneous enough to provide high values of heat transfer conductivity in comparison with a fixed bed composed only with salt grain. The implementation characteristics of such a reactive composite medium (proportion of constituents, mixing protocol of the constituents, apparent density of the mixture, etc.) have a strong effect on the quality of the heat and mass transfers as well as on the texture of these composite media. The composition must be carefully optimised in accordance with the targeted energy and power density that must be reached.

Deliverable D4.1 aims to give general indications for the optimisation of such a salt/graphite reactive compound (TCM) in order to achieve compact heat storage units with high energy density (at least 200 kWh heat /m³ and 80 kWh cold). This optimisation focusses on the choice of the best composition salt/ENG of the reactive compound, in order to reach acceptable power levels (heat and cold powers) during the different operating phases of the TCM storage unit. Once the reactive medium is characterised, the design and dimensioning of the reactor is then carried out. The development of a simplified steady state model of a compressor-assisted thermochemical unit will help to analyse the parameters that impact the design of the TCM reactor in order to optimise in accordance with the operating conditions, the thermal needs of the building or the thermal energy resource provided that can be stored into chemical form into the TCM unit.

This deliverable is divided in three main parts:

1. A first section of this report (parts 1 to 3) presents briefly the principal of thermochemical storage process and the study of 2 potential salts CaCl₂ or BaCl₂ that can be used for the Ministor TCM unit.
2. A second section of the document describes a numerical study of TCM reactive material. The objective here is to define the suitable implementation parameters in order to avoid limitations by heat and mass transfer inside the reactive material.
3. The final section focusses on the development of steady state model of the TCM reactor coupled with an ammonia compressor during the charging phase. The aim of this section is to give an optimal design of the reactor and also to understand how the solar thermal power delivered to the TCM reactor impacts the choice of the ammonia compressor.

2. Choice of the reactive salts per operating conditions

The first step in the development of such a thermochemical storage system is the choice of the reactive salt capable of reacting with ammonia and meeting the operating conditions that are seasonally variable. Ammonia was chosen as the refrigerant as it meets the requirements for the development of an environmentally safe system. The use of water as refrigerant is not possible in this application as it requires very low (vacuum) operating pressures. This choice nevertheless imposes some security constraints as it is toxic at very low concentration in the air. The use of ammonia has the advantage of being readily available, inexpensive, does not contribute to ozone depletion, greenhouse effect or global warming, and is biodegradable. However, its toxicity requires unique safety measures to be taken. Since ammonia reacts with copper, ammonia systems must be built using aluminium or stainless-steel material.

The two processes, i.e., the chemical reaction and the phase-change are mono-variant and their thermodynamic equilibrium conditions follow the Clausius–Clapeyron (pressure-temperature) relation. The equilibrium conditions for the two processes are determined by only one variable, either pressure or temperature:

$$\ln\left(\frac{P_{i,eq}}{P_{ref}}\right) = -\frac{\Delta H_i^0}{R \cdot T_{i,eq}} + \frac{\Delta S_i^0}{R}, \quad i = \begin{cases} r : \text{reaction} \\ \text{liq-vap} : \text{liquid-vapor} \end{cases}$$

where $P_{i,eq}$ and $T_{i,eq}$ correspond to the equilibrium pressure and temperature of each process (either reaction, either L/V phase change), ΔH^0 and ΔS^0 are the standard enthalpy and entropy of the two processes and P_{ref} is a standard reference pressure (generally 1 bar).

The selection of the reactive salt is made, first, based on temperature /pressure equilibria of the reactions between the salt and ammonia and in accordance with the operating conditions. Once the reactive salt has been selected, it is then to be implemented and placed in such way in a fixed bed thermochemical reactor as to give it appropriate heat and mass transfer properties. Knowledge of the physico-chemical properties of reactive salt and transfer parameters are necessary to design the TCM storage unit for a given application. A pre-selection of reactive salt has been carried out according to the energy density and the position of the equilibrium curves. These must be within temperature and pressure ranges corresponding to the operating conditions imposed by the application.

- **The (P,T) equilibrium curve**, plotted in $(\ln(P)); -1/T$ diagram, also called Clausius-Clapeyron diagram, must be in accordance with the desired operating conditions:
 - In winter, the charging phase uses the solar heat that can be delivered at least at 55/60°C. The heating effect provided by the reactor the TCM storage unit during the discharging phase has to be around 50/55°C, while outside temperature is about -5°C /+5°C.
 - In summer, the charging phase uses the solar heat that can also be delivered at least at 65°C. The cooling effect provided by the evaporator of the TCM storage unit during the discharging phase has to be is around 0°C, while outside temperature is about +35°C.
 -

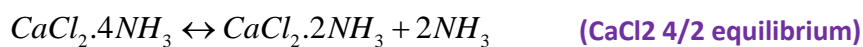
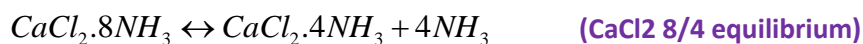
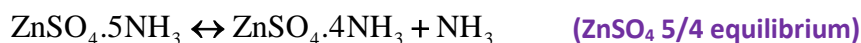
- **Energy density** of the reactive salt must be as high as possible in order to obtain reasonable masses and volumes of reactive material. A minimum storage density of 200 kWh/m³ of reactive material must be reached according the Ministor energy target to be met. When the salt is fully ammoniated, an effective porosity of the TCM material has to remain in order to ensure a satisfactory diffusion of the reactive gas into the reactive material. This effective porosity limits the amount a salt that can be implemented into a given TCM reactor volume and thus the maximum energy density of the TCM material, which can be defined **in first approximation** (the calculations of the energy density are more precisely carried out later) as:

$$De_{\max} \approx \frac{v \cdot \Delta H_R^\circ \cdot (1 - \varepsilon)}{Vm_{\text{salt_full}}} \quad [kW/m^3 \text{ of TCM material}]$$

where v is the stoichiometric coefficient of the reaction, ΔH_R is the enthalpy of reaction, ε is a minimum required porosity assumed to be around 0.2 in first approximation, $Vm_{\text{salt_Full}}$ is the molar volume of the fully ammoniated salt,

- **Reactivity:** The reaction must be completely reversible, i.e., no loss of reactivity during numerous decomposition / synthesis reactions cycles. To ensure reproducible performance and durability of the system, at the end of each cycle, the reactive salt must be in the same state as at the beginning of the cycle (same quantity of gas exchanged in synthesis and decomposition). The kinetics of the reaction must be fast enough to allow significant powers and be able to link the phases of synthesis and decomposition quickly. In addition, the salt must have good physical and chemical stability in order to achieve the storage function without loss of its potential, it must not be subject to degradation such as sintering, which can appear if the operating temperature is too close to its melting temperature. Sintering reduces the specific surface area and thus the reactivity.
- **Energy storage cost :** The cost of salt is also crucial in the choice of salt to be used, as it directly impacts the cost of the stored kWh and therefore the economic viability of the TCM storage unit.

In accordance with the operating conditions, several ammoniated salts have been selected. The corresponding reactions are as follows:



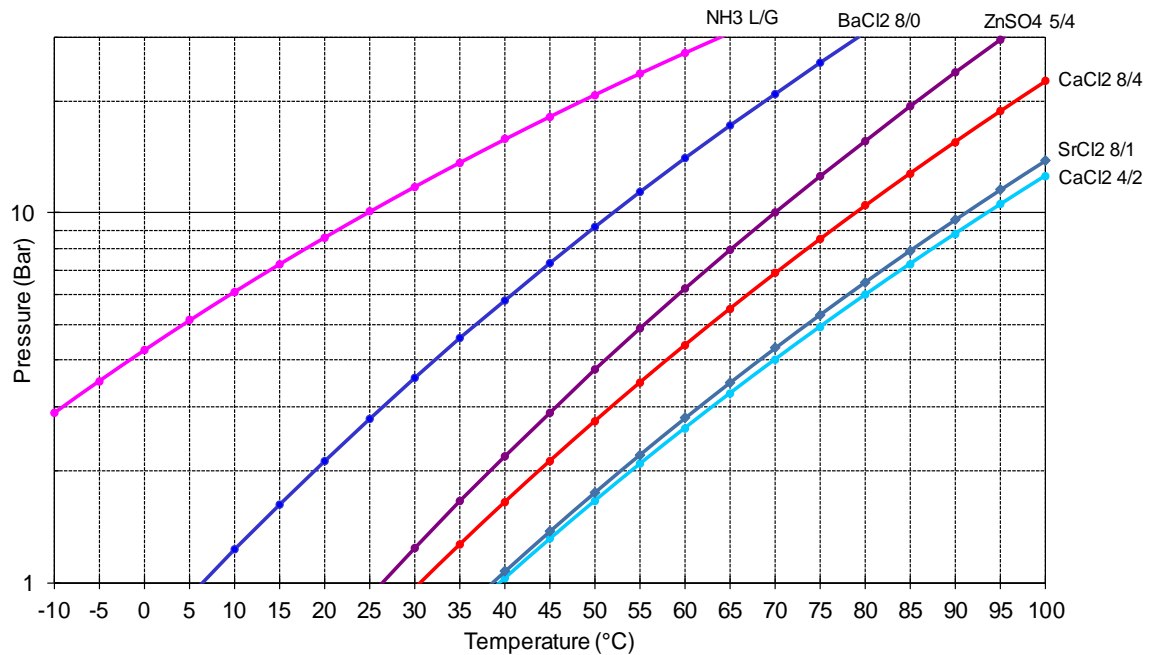


Figure 3 : Equilibrium reaction curves of some ammoniated salts that can be considered for low temperature storage application such as Ministor storage

The following table shows as a first approximation the energy densities of the TCM material as well as the cost of the stored energy using the different selected salts and considering a remaining porosity of 20% for the TCM material when the salt is fully ammoniated:

Table1 : Energy density and cost of the energy stored for the selected salts :

Considered reaction	BaCl ₂ 8/0	ZnSO ₄ 5/4	CaCl ₂ 8/4 + 4/2	SrCl ₂ 8/1
Enthalpy of reaction ΔH_r [J/mole of G]	38250	45198	42300	41430
Stoichiometric coefficient ν	8	1	6	7
Molar volume of the fully ammoniated salt	$225 \cdot 10^{-6}$	$210 \cdot 10^{-6}$	$207 \cdot 10^{-6}$	$212 \cdot 10^{-6}$
Amount of salt [mole/m ³ of TCM material]	3333	3571	3623	3537
Energy density [kWh/m ³ of TCM material]	302	47	272	304
Cost of hydrated salt [€/kg hydrated salt] (hydration state of commercialized salt)	25 (@2H ₂ O)	15 (@7H ₂ O)	0.70 (@2H ₂ O)	220 (@6H ₂ O)
Cost of 1 mole anhydrous salt [€/mole salt]	6.1	4.3	0.1	58.8
Cost of stored energy [€/kWh]	71	342	1.40	729

As it can be seen in Table 1, ZnSO₄ salt cannot achieve the energy density targeted in the project and is therefore discarded. Furthermore, even if the equilibrium curve position of the reaction involving the SrCl₂ salt can meet the operating requirements of Ministor system, the cost aspects have also to be taken into account: SrCl₂ salt leads to a too high cost of the stored energy (10 times higher than BaCl₂ and 500 times higher than CaCl₂) and thus this salts was also discarded.

Following this, only two of the selected salts can suit the Ministor application: BaCl₂ and CaCl₂ salts.

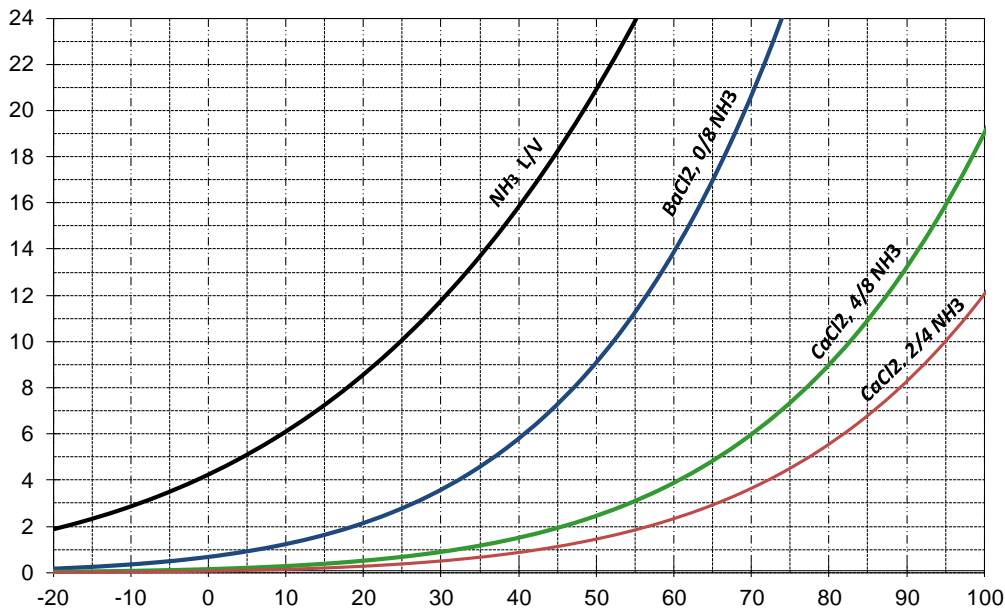


Figure 4 : (P-T) diagram of the reaction equilibria that can be considered for Ministor $BaCl_2 \cdot (8/0)NH_3$, $CaCl_2 \cdot (8/4)NH_3$, $CaCl_2 \cdot (4/2)NH_3$ for TCM unit, and L/V phase-change of ammonia.

For the $CaCl_2$ salt, it can be seen in Figure 4 that 2 equilibria very close to each other (around 10K from each other) are possible to exploit. If only the first reaction (8/4) is exploited then the maximum storage density is only about 180 kWh/m³, which is lower than the targeted energy density for the TCM unit. Therefore, it will also be necessary to exploit the second reaction to reach the initial objectives that have been set. Indeed, if this second reaction (4/2) is also exploited completely, then it will be possible to reach a maximum energy density of 272 kWh/m³ of TCM material considering a residual porosity of 20% when the salt is completely ammoniated to 8 mole of ammonia. Thus, as will be seen later, the energy density of the TCM unit is flexible and can be adjusted from 180 kWh/m³ to 270 kWh/m³ just by partially exploiting the second reaction.

3. TCM system configurations using a thermochemical reactor implementing either BaCl₂ or CaCl₂ salt.

3.1 Winter operating mode (heating)

3.1.1 Storage mode:

On a winter day, the PVT provides heat at 60°C that is used to desorb the salts and the heat of condensation released at 25/30°C by the TCM unit is used by the evaporator of the HP in order to upgrade it at 65°C and store it into the hot PCM at around 58°C. Depending on the TCM salt that will be used, this step may not require the use of a compressor. Indeed, if BaCl₂ is used no NH₃ compressor is needed as the heat is provided by the PVT at a high enough temperature to drive the decomposition at the pressure imposed by the condenser. If CaCl₂ is used, then a NH₃ compressor is mandatory in order to run this decomposition.

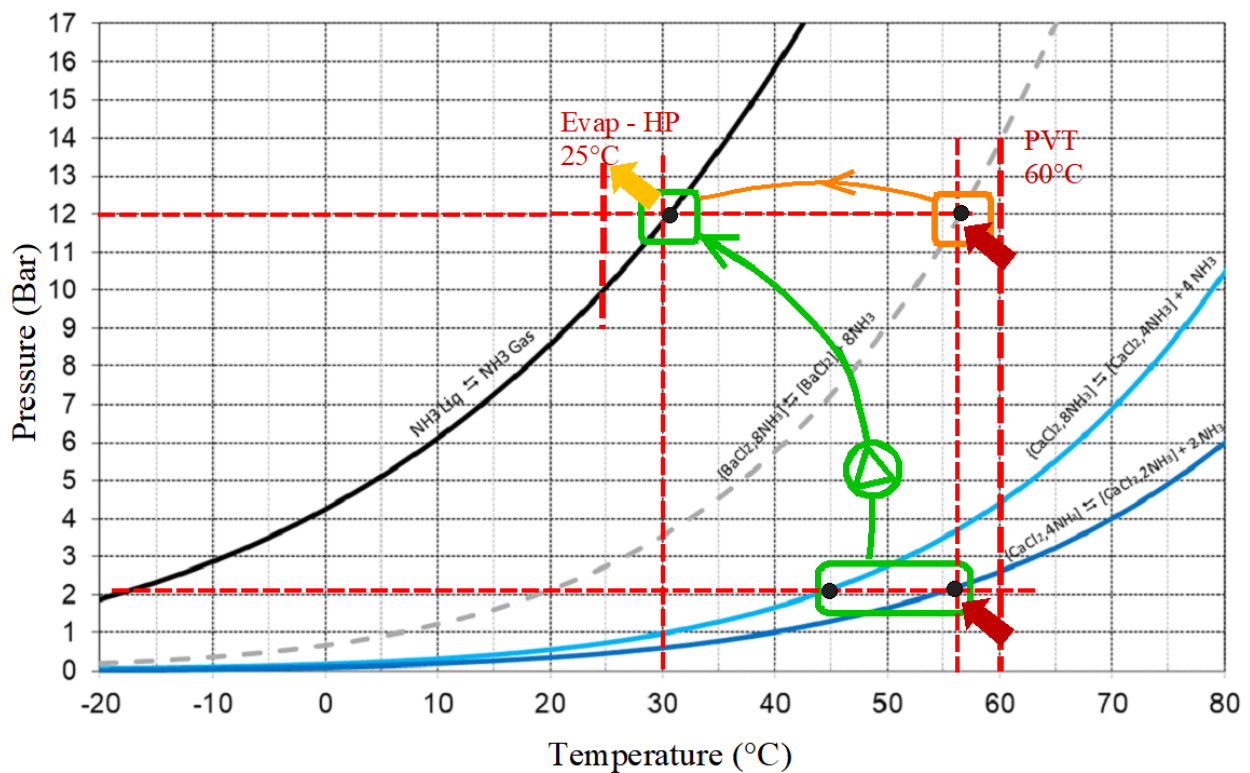


Figure 5 : Thermodynamic operating conditions [Pressure (Bar) / Temperature (°C)] of TCM storage unit in **Storage mode** in winter

3.1.2 Discharge mode:

On a winter night, the evaporator of the TCM unit pumps outside heat at $-5^{\circ}\text{C}/0^{\circ}\text{C}$ (evaporator at $-10^{\circ}\text{C}/-5^{\circ}\text{C}$). The NH_3 vapour produced by the evaporator is absorbed by the reactive salt into the reactor. If CaCl_2 is implemented, the TCM unit can produce the heat of reaction at 50°C which can be enough for the heating need. If BaCl_2 is used, the heat of reaction is produced only at $20^{\circ}\text{C}/25^{\circ}\text{C}$, which is not enough for the heating purpose during night, unwise if it is upgraded by the HP, as it is done for the upgrading of the condensation heat during the storage step. In this case, the HP will operate only during the day if CaCl_2 is used or only during the night if BaCl_2 is used. We must choose what is the most relevant for the project.

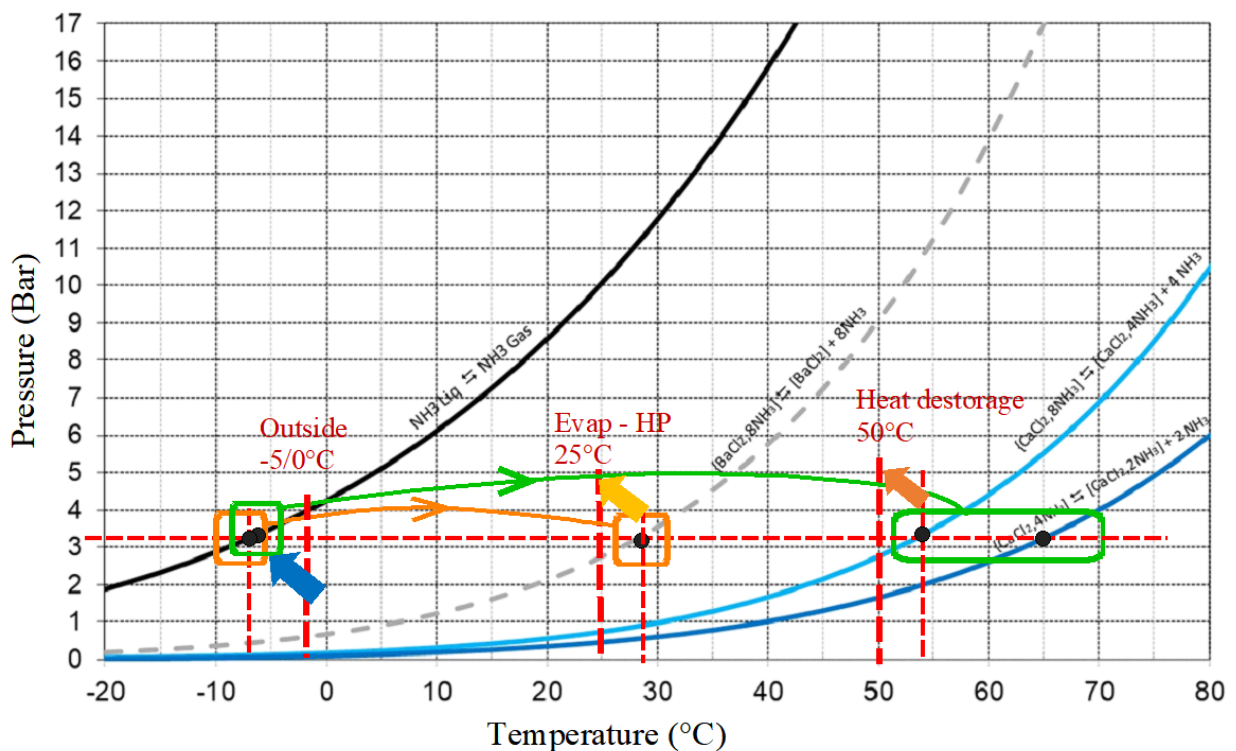


Figure 6 : Thermodynamic operating conditions [Pressure (Bar) / Temperature ($^{\circ}\text{C}$)] of TCM storage unit in **Discharge mode** in winter (Heating mode)

3.2 - Summer operating mode (cooling mode)

3.2.1 Storage mode:

During hot summer day, the PVT provides heat at 65°C or more. If BaCl₂ is used, this temperature level is enough to drive the decomposition and does not require NH₃ compressor, even if the condensation takes places at 50°C with an outside temperature of 35°C. If CaCl₂ is used, a NH₃ compressor is then needed to make possible the decomposition of the salts (with a compressor ratio of 6).

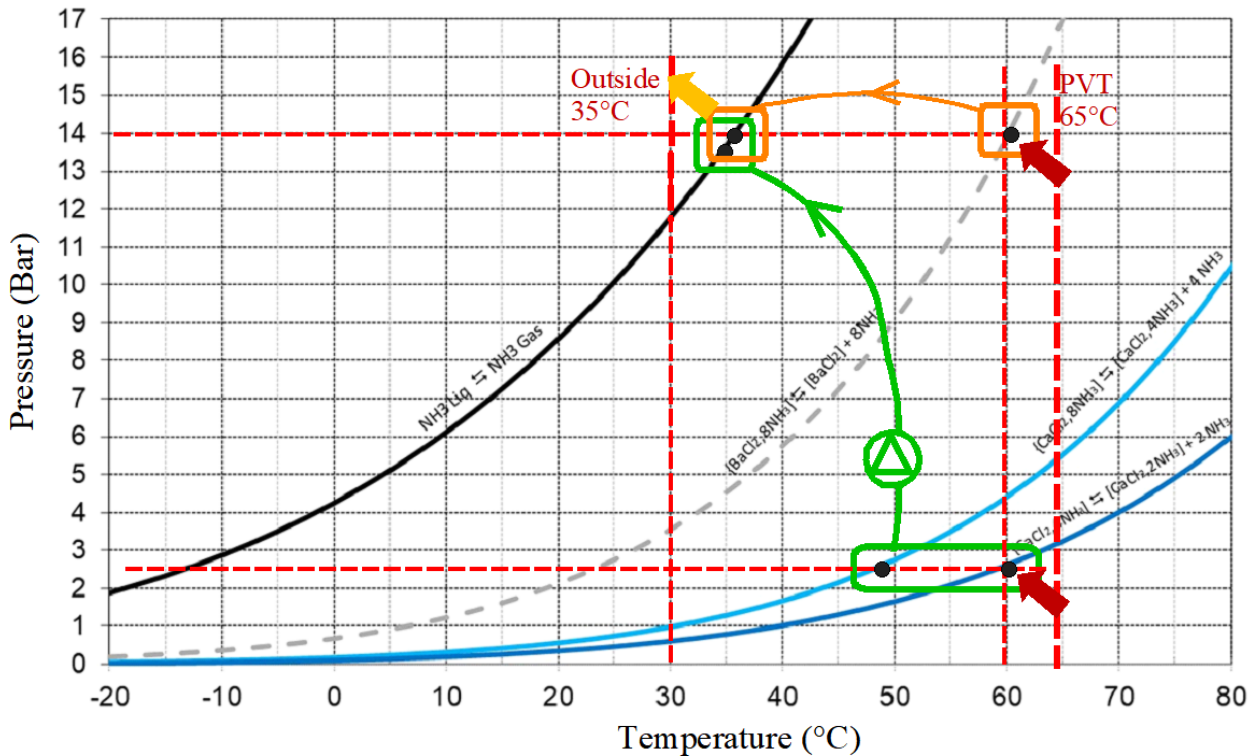


Figure 7 : Thermodynamic operating conditions [Pressure (Bar) / Temperature (°C)] of TCM storage unit in **Charging mode** in summer

3.2.2 Discharge mode:

If CaCl₂ is used, the cold production is possible at even very low temperature (from 0°C to - 20°C). If BaCl₂ is used, the cold production temperature may be effected by the outside temperature. If outside temperature is higher than 30°C, the cold is also produced at higher temperature and may be greater than the cold temperature required for the cold PCM storage. Otherwise, a cold PCM with a higher melting temperature is required or the use of a NH₃ compressor (pumping the vapour of the evaporator) may be used to adapt the working condition of the reactor on the outside temperature.

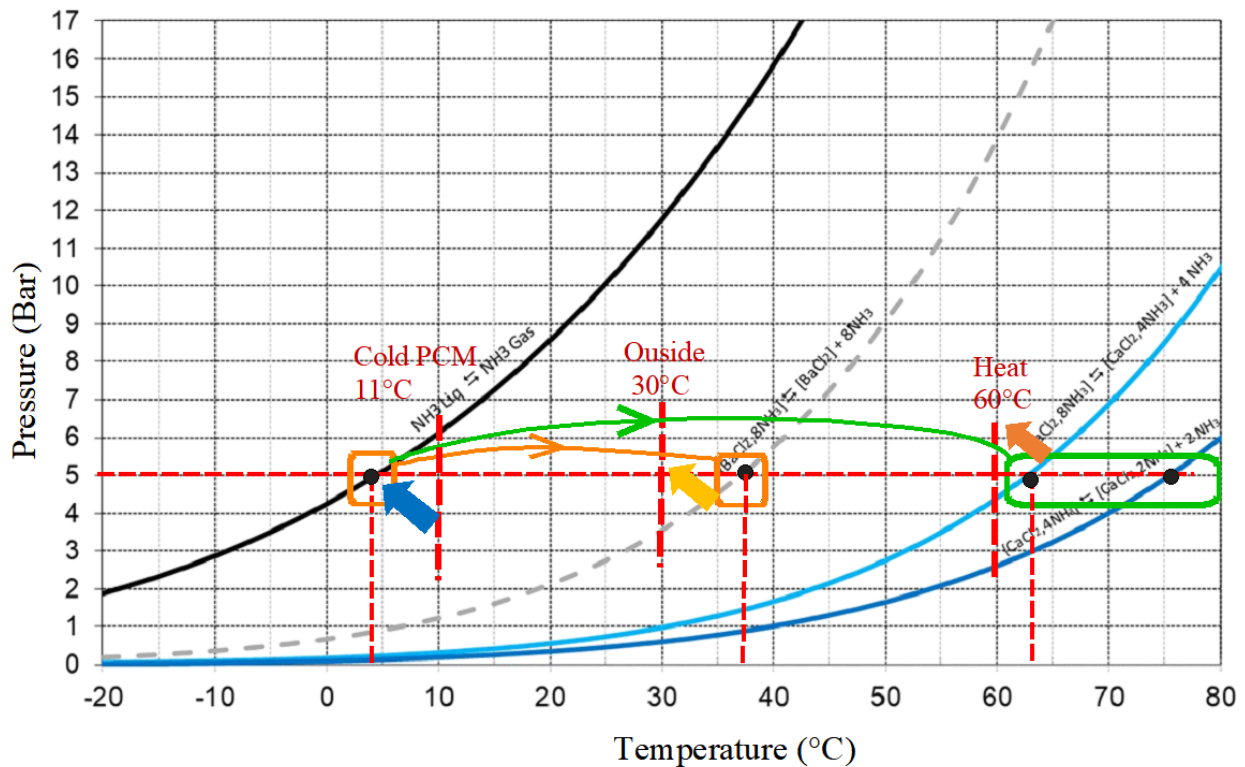


Figure 8 : Thermodynamic operating conditions [Pressure (Bar) / Temperature (°C)] of the TCM storage unit in **Discharging mode** in summer (Cooling mode)

3.3 – Choice of the reactive salt

During winter, the BaCl_2 -based TCM discharges heat at only 20-25°C and thus, needs to use a heat pump to upgrade this heat at 65°C, a suitable temperature for the PCM storage. This solution may be relevant if the discharge operation is carried out during the day in order to consume the electricity produced by the PVT, instead of using the stored electricity during the night. To implement this solution (discharge during the day), two TCM units are required, each one operates during the day, one in storage mode the other in discharge mode. In these two operating mode, the heats released at 20-25 °C by the condenser in storage mode and by the reactor during the discharge mode are both used by the evaporator heat pump which upgrade it at 65°C. This TCM implementation that avoids using a NH_3 compressor by requiring a night and day operation of the heat-pump, is of interest, and needs further study and assessment.

During summer, the heat delivered by the PVT is enough for the BaCl_2 based TCM without using the NH_3 compressor. The cold produced by the system during the night can be delivered at a temperature suitable for the cold PCM only if the outside temperature is not too high (preferably lower than 30°C). If higher outside temperatures occur, the BaCl_2 -based system will produce cold at a higher temperature and then the PCM may not solidify. In this climatic case, a higher melting temperature for the cold PCM must be chosen.... So, the choice of BaCl_2 or CaCl_2 salts must be considered. While the BaCl_2 choice may avoid the use of a compressor, the heat produced by the TCM in winter would always need to be upgraded by the

heat pump and the cold produced at the evaporator in summer may not be enough to make solidify the PCM as the reactor is not sufficiently cooled because of the high outside temperatures.

Taking these considerations into account, it has been decided to choose calcium chloride salt, CaCl_2 , which reacts with two, four or eight moles of ammonia (NH_3) to form the ammoniated salts $\text{CaCl}_2 \cdot 8\text{NH}_3$, $\text{CaCl}_2 \cdot 4\text{NH}_3$ and $\text{CaCl}_2 \cdot 2\text{NH}_3$ that are reacting reversibly with each other according to the reactions of Table 2.

Table 2 – Characteristics of ammoniated calcium chloride salts and corresponding reaction

	First reaction $\text{CaCl}_2 \cdot 8\text{NH}_3 \leftrightarrow \text{CaCl}_2 \cdot 4\text{NH}_3 + 4 \text{NH}_3$		Second reaction $\text{CaCl}_2 \cdot 4\text{NH}_3 \leftrightarrow \text{CaCl}_2 \cdot 2\text{NH}_3 + 2 \text{NH}_3$	
Heat of reaction (J/mole NH_3)	42433		42145	
Entropy of reaction (J/mole NH_3)	235.4		229.5	
Maximal Energy storage density of salt (Wh/kg anhydrous salt)	820		634	
Ammoniated salt densities (kg/m ³)	$\text{CaCl}_2 \cdot 8\text{NH}_3$ 1193	$\text{CaCl}_2 \cdot 4\text{NH}_3$ 1380	$\text{CaCl}_2 \cdot 2\text{NH}_3$ 1606	CaCl_2 2172

4. Implementation characteristics of the TCM reactive material

The key issues with the reactive media used in thermochemical reactors lies in their capacity to transfer the heat of reaction from or to the reactor wall (thermal conductivity λ , thermal contact resistance at the wall h_{sw}) and to their ability to diffuse the reactive gas (permeability k , gas diffusivity D) in all the reactive material without too much pressure drop from or to the reactor inlet. The power performance of thermochemical reactors is highly dependent on the quality of the heat transfers and reactive gas diffusion in the porous reactive material used in these reactors.

A reactive medium made up of salt alone has very low thermal conductivity (less than $0.5 \text{ W/m}^2 \cdot \text{K}$), and thus strongly limits heat transfer in the reactive bed. This low thermal conductivity implies long reaction times and therefore very low reaction powers. The addition of a third body such as the Natural Expanded Graphite (ENG), which is a very good thermal conductor, significantly increases the apparent conductivity of the reactive bed. Such an implementation has been realised for the first time at CNRS-PROMES laboratory in 1981 and patented in 1983¹². Several theses at the CNRS laboratory have been devoted to the study of the behaviour of such salt/ENG reactive composites, and how implementation way of such composite affects the heat and mass characteristics that moreover evolve during the reaction. The mastering of implementation parameters is crucial to maximise their specific performance, such as the power density or energy density of the material.

The porous reactive material developed for many years in CNRS Laboratory is a mixture of reactive salt and expanded natural graphite, which is afterwards consolidated by mechanical compression either in a mould or directly into the reactor tube. The material obtained is a highly porous composite, with an enhanced thermal conductivity conductor and with a certain elasticity capable of absorbing the swelling of the reactive salt over the reaction.

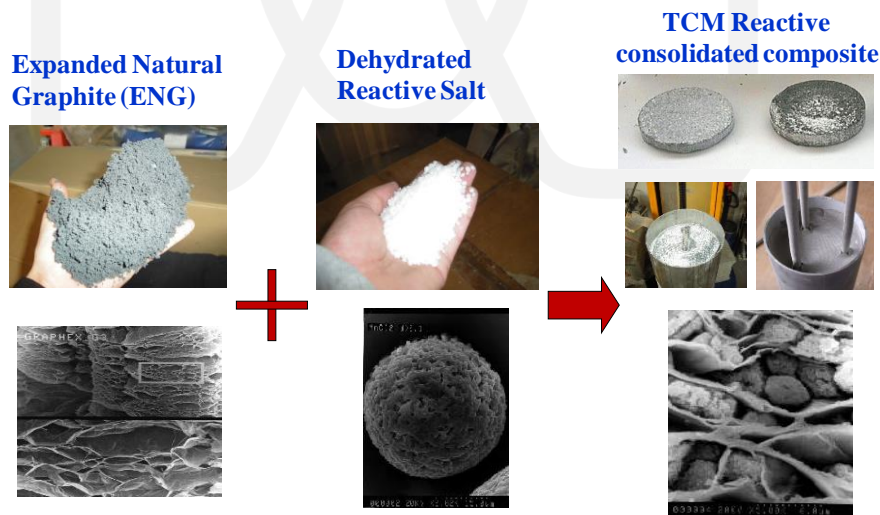


Figure 9: Raw materials used for the TCM reactive composite and obtained in situ compressed mixture of expanded graphite and anhydrous salt

The expanded graphite (ENG) is in the form of a worm-type particle (of the order of a cm) with a low bulk density (3 to 4 kg/m^3). The choice of this graphite binder is justified by its high intrinsic conductivity of the order of $200\text{-}400 \text{ W/m}\cdot\text{K}$, its extreme porosity (97 to 99.9%) and its mechanical properties, in particular

¹ Coste C, Mauran S, Crozat G. Gaseous–solid reaction. US Patent 4595774, 1986.

² Olives R, Mauran S. A highly conductive porous medium for solid–gas reactions. Effect of the dispersed phase on the thermal tortuosity Transport in Porous Media 2001;43(2):377–94

its elasticity. Its quality is strongly dependent on the origin of the precursor material enabling to obtain the ENG: the graphite-intercalated compound (GIC) which is presented in the form of graphite flakes in which a mixture of nitric acid and sulfuric acid is inserted. The CNRS laboratory has acquired a strong experience on the exfoliation of this CIG in order to obtain, after exfoliation at 1000°C, good quality ENG worm-type particles with an apparent density of 2.5-3.5 kg/m³ and with a mean size of the worm-type particles between 10 and 20mm. An exfoliator was built in the laboratory in 2002-2003 to produce our own ENG. Nevertheless, natural expanded graphite can be bought from different suppliers (IMERYS, Graphite Kropfmühl, ...). It must be pure (carbon content > 99%), highly exfoliated (density of 3 kg/m³) with worm-type particle length greater than 10 mm.

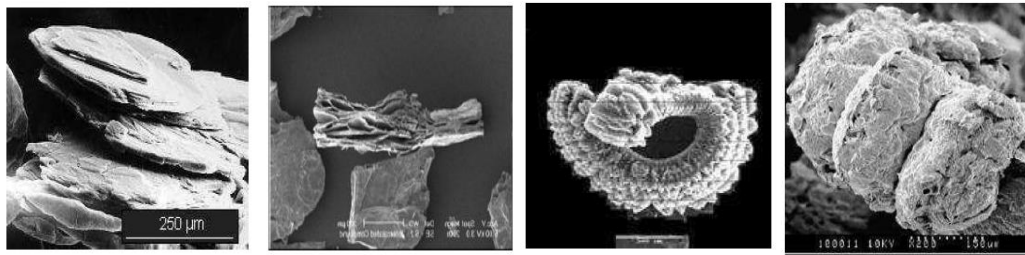


Figure 10 : Natural graphite flakes, Intercalated graphite flakes and Expanded ENG worm

The reactive salt (CaCl_2) is generally bought in dihydrate form ($\text{CaCl}_2 \cdot 2\text{H}_2\text{O}$) and it need absolutely to be completely dehydrated before making it react with ammonia. For this reason, a ventilated oven is required to dehydrate the salt. This dehydration is proceeded in 2 steps.

Firstly, the raw salt is placed in trays for 24 hours at 200°C to remove the water content until to reach the $\text{CaCl}_2 \cdot 1/3\text{H}_2\text{O}$.

Once the salt has been firstly partially dehydrated in the ventilated oven, it has then to be grinded and milled to obtain a powder with a granulometry of about 100μm. Different grinder may be used, the suitable one is centrifugal type with sieve. After the salt has been milled, it must be hermetically bagged while waiting to be mixed with the GNE.

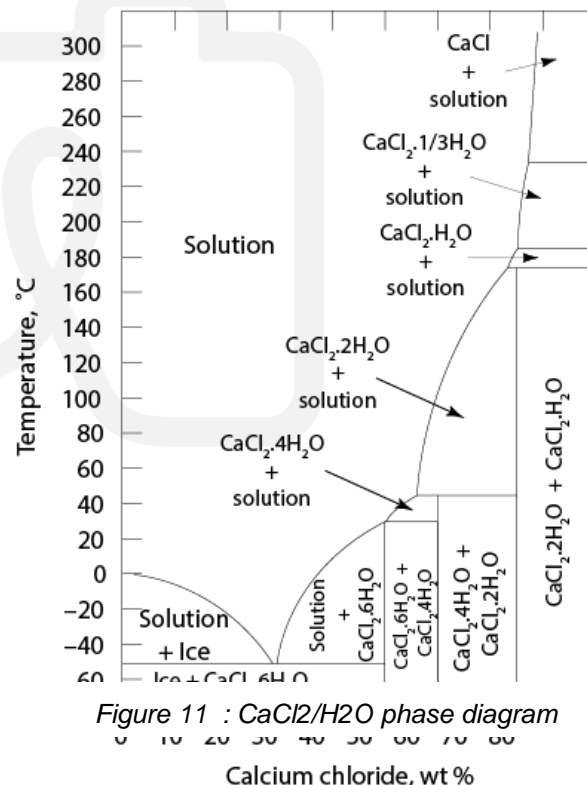


Figure 11 : $\text{CaCl}_2/\text{H}_2\text{O}$ phase diagram

To remove the last water content from the salt, a

second dehydration is carried then out when the composite has been placed into the reactor tube, which is then completely sealed. The heating of the reactor tube at 200°C connected to a vacuum pump enables the removal of the last water content in salt.

To avoid corrosion of the tube in which the calcium chloride is placed, the salt is strongly in situ dehydrated and always kept in a solid state (salt). Indeed, corrosion phenomena mainly occur when the salt is solubilised in liquid ammonia or water and in the presence of oxygen. These situations never occur because the reactor tube filled with salt is first evacuated (no oxygen remains) and the solubilisation of

the salt is avoided by controlling the pressure of the reactor during operation: this must never be higher than the pressure of the saturated solution (about the half that of the liquid/vapour phase change of ammonia). Furthermore, the material of the reactor tube is made of stainless steel, the **grade 316L (EN 1.4435)**, which is one of the most cost-effective and corrosion-resistant stainless steel. The significant presence of molybdenum (about 3%) in the 1.4435 stainless steel is well known to increase the corrosion resistance to chlorides, strong acids and bases.

4.1 Characteristics of the ENG/Salt composite TCM material

The TCM reactive medium is a compressed mixture of the dehydrated salt (CaCl_2) with the expanded natural graphite binder (ENG). After consolidation by compression, the composite block forms a porous structure consisting of a matrix of stacked ENG sheets with a preferential orientation perpendicular to the direction of compaction, and between which the salt grains are uniformly dispersed. This particular foliar structure is therefore conducive to a good heat transfer in the radial direction towards the reactor wall where the heat is exchanged with a heat transfer fluid. This porous material can be schematised as follows

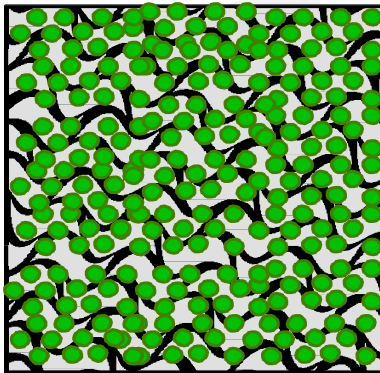


Figure 12: Schematic view of the salt/ENG composite

The mass of the resulting composite block (M_{comp}) is defined by the sum of the mass of salt and graphite:

$$M_{comp} = M_{salt} + M_{graph}$$

and its apparent volume of the composite V_{comp} can be considered as the sum of the volumes occupied by the solid matter corresponding to graphite (V_{graph}) and salt (V_{salt}), the remainder being the void volume (V_{void}):

$$V_{comp} = V_{graph} + V_{salt} + V_{void}$$

We can define various parameters to characterize in a relatively relevant way such a composite implementation:

- τ_s : the mass ratio of salt (by convention anhydrous) in the mixture defined as:

$$\tau_s = \frac{M_{salt_anhydrous}}{M_{comp}} \quad (\text{kg of anhydrous salt / kg of composite})$$

- The density the obtained composite reactive material

$$\rho_{Comp} = \frac{M_{Comp}}{V_{comp}} \quad (\text{kg/m}^3 \text{ composite})$$

- The apparent density of the Expanded Natural Graphite in the composite material

$$\rho_{ENG} = \frac{M_{graph}}{V_{comp}} = (1 - \tau_{sel}) \cdot \rho_{comp} \quad (\text{kg of ENG / m}^3 \text{ of composite})$$

- The maximal energy density (De_{max}) of the reactive material (considering that all the ammoniated salt $CaCl_2 \cdot 8NH_3$ has been completely decomposed into $CaCl_2 \cdot 4NH_3$ (De_{max1}) and additionally if the latter is also completely decomposed into $CaCl_2 \cdot 2NH_3$. As it can be seen ($De_{max1\&2}$), the addition of ENG reduces the energy storage density of the composite, which is directly related to the implemented mass of salt. As we can see in the figure 12, the energy density of the material increases with salt mass ratio and with the apparent density of the ENG in the TCM reactive composite material.

$$De_{max1} = \left(4\Delta H_{R1}^o\right) \frac{\tau_s \rho_{comp}}{Mm_{anhydr}} \quad (\text{kWh/m}^3 \text{ of composite})$$

$$De_{max1\&2} = \left(4\Delta H_{R1}^o + 2\Delta H_{R2}^o\right) \frac{\tau_s \rho_{comp}}{Mm_{anhydr}} \quad (\text{kWh/m}^3 \text{ of composite})$$

where the quantity $n_{salt} = \frac{\tau_s \rho_{comp}}{Mm_{anhydr}}$ characterizes the number of moles of salt contained in $1m^3$ of composite

The actual energy density De of the reactive material that is obtained practically depends on the desired (or achievable) advancements rate for each considered reaction ΔX_1 and ΔX_2 and thus are reduced in comparison of the previous maximal densities, as defined below:

$$De = \left(4.\Delta X_1.\Delta H_{R1}^o + 2.\Delta X_2.\Delta H_{R2}^o\right) \frac{\tau_s \rho_{comp}}{Mm_{anhydr}}$$

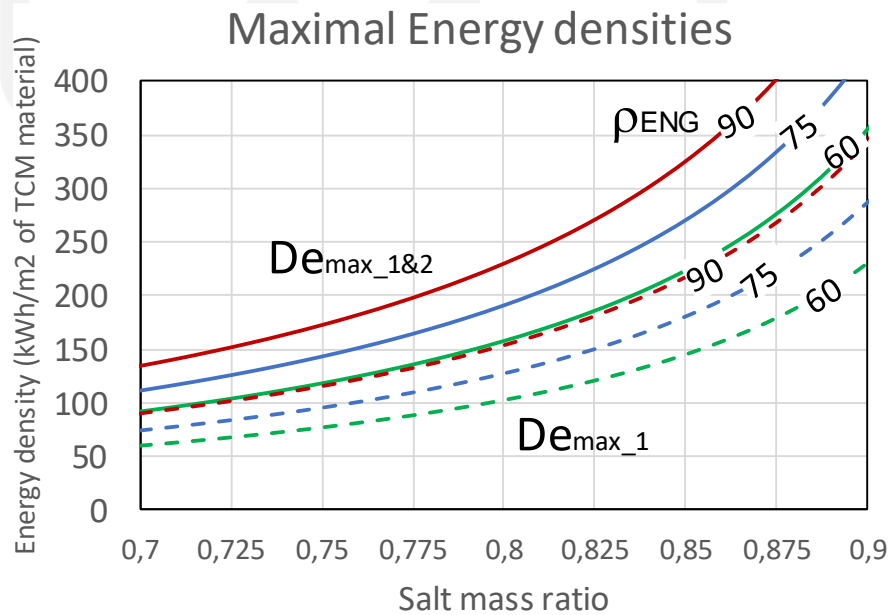


Figure 13: Maximum energy density of the TCM material considering either the 1st reaction or the 1st and 2nd reaction, as a function of the salt mass ratio and apparent bulk density of ENG in the TCM material

The **porosity of the composite material** is of importance and can be determined from these implementation parameters. Porosity characterises the pore volume in the material and has a strong effect as we will see later, on the quality of the transfers, in particular the diffusion of the reactive gas in the matrix. This porosity is defined as the ratio of the void volume to the total volume of the composite and is therefore a function of the volume occupied by the different solid phases that are graphite and salt.

The volume occupied by graphite can simply be expressed from the density of pure graphite ρ_{graph}^* of 2250 kg/m³. The volume V_{salt} occupied by the salt is, on the other hand more difficult to determine because it varies during the reaction. It can however be evaluated from the number of moles of salt implemented in the composite and the molar volume $Vm(X)$ of the salts which varies with the advancement rate X of the reaction. Then, it results the final expression of the TCM material porosity for a given state of charged of the reactive salt:

$$\varepsilon = \frac{V_{void}}{V_{comp}} = 1 - \frac{V_{graph}}{V_{comp}} - \frac{V_{salt}(X)}{V_{comp}} = 1 - (1 - \tau_s) \frac{\rho_{comp}}{\rho_{graph}^*} - \frac{\tau_s \rho_{comp}}{Mm_{anhydr}} \cdot Vm(X)$$

The following graphs shows how the porosity of the TCM composite material when the salt is fully charged at 8 moles of ammonia ($CaCl_2 \cdot 8NH_3$) evolves as a function the apparent density of ENG and the salt mass ratio. This porosity decreases strongly with increasing values of salt mass ratios and apparent bulk density of ENG.

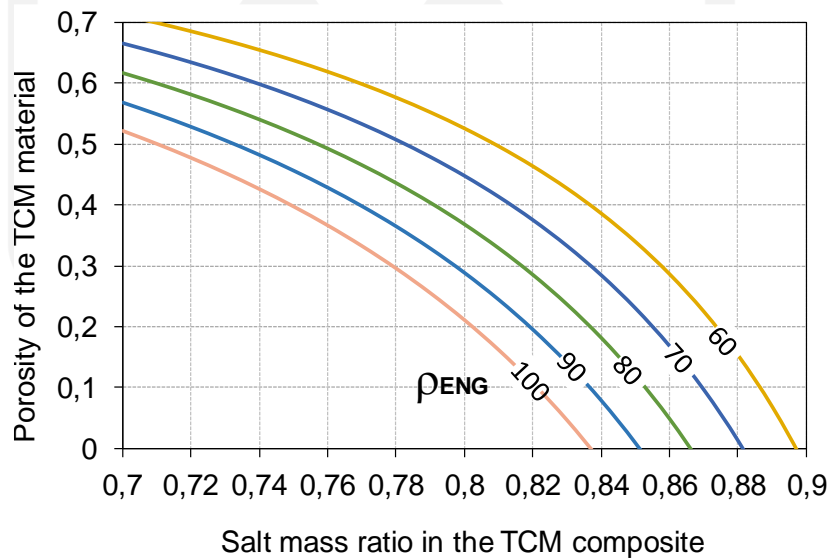


Figure 14: Evolution of the porosity of the TCM composite material when fully charged with ammonia ($CaCl_2 \cdot 8NH_3$), as a function of the apparent ENG density and salt mass ratio

As it will be seen later, the porosity of the material has a strong impact on the permeability of the reactive material and thus the diffusion of the reactive gas through it. A minimum porosity (about 20%) is then required in order to avoid a reaction limitation by mass transfer in the reactive material.

4.2 Heat transfer and mass transfer characteristics of the TCM reactive material

Studies³ that have been carried out in CNRS laboratory have showed that the thermal conductivity of these consolidated reactive blocks is closely correlated to the apparent density of graphite in the composite matrix (generally varying from 50 to 120 kg of ENG/m³ composite) and to a lesser extent by the mass ratio of anhydrous salt in the matrix. It also changes only very little during the reaction. The radial effective thermal conductivity $\lambda_{comp\ rad}$ can be estimated in a simple way by the following linear relation for this low apparent ENG density range (50- 100 kg of ENG/m³ composite):

$$\lambda_{COMP\ rad} = 0.08\rho_{ENG}$$

While ENG is an ideal binder for intensifying heat transfer and absorbing the swelling of the salt, it is however much less efficient for mass transfer. Indeed, the reactive composites used in the TCM reactors must be sufficiently porous to allow an ease diffusion of the reactive gas to the salt. This porosity is affected, as we have previously expressed, by the presence of ENG which is necessary to improve heat transfer and absorb the variations in volume of the reagent during the reaction. Numerous studies that have been carried at PROMES laboratory⁴⁵ have enabled correlation of the diffusivity and permeability of the reactive composite material with the implementation parameters. It seems that the most relevant parameter to characterize these mass transfer characteristics in these consolidated salt/ENG mixtures is the effective bulk density $\rho_{lex(X)}$ defined as the ratio of the mass of ENG in the composite to the volume occupied by the graphite and the void volume. This particular effective density varies with the progress of the reaction.

$$\rho_{lex(X)} = \frac{M_{ENG}}{V_{graph} + V_{void}} = \frac{M_{ENG}}{V_{comp} - V_{salt}(X)} = \frac{1}{\frac{1}{\rho_{graph}^*} + \frac{\epsilon(X)}{\rho_{GNE}}} \quad \text{with } \rho_{graph}^* = 2250 \text{ kg/m}^3$$

The permeability k , which then also varies with the conversion rate of the salt, can then be correlated to this parameter by the empirical expression:

$$k_{(X)} = \frac{C}{\rho_{lex(X)}^n}$$

where constant C and exponent n have been experimentally identified at $C=7.10^{-5}$ and $n=3.7$ for various ENG /salt composites with different salt mass ratios (ranging from 60 to 85%) and ENG densities (ranging from 50 to 120 kg/m³).

The following graphs shows how evolved the permeability is with the final porosity of the fully charged TCM material containing different anhydrous salt mass ration. From the experience of the CNRS

³ Olivès, R et S Mauran. "A Highly Conductive Porous Medium for Solid–Gas Reactions: Effect of the Dispersed Phase on the Thermal Tortuosity." *Transport in Porous Media* 43 (2001):377-394.

⁴ S. Mauran, P. Prades, F. L'Haridon, Heat and mass transfer in consolidated reacting beds for thermochemical systems, Heat Recovery Systems and CHP, 13 (4), pp. 315-319, 1993.

⁵ S. Mauran, L. Rigaud, O. Coudeville, Application of the Carman–Kozeny Correlation to a High-Porosity and Anisotropic Consolidated Medium: The Compressed Expanded Natural Graphite, *Transport in Porous Media*, 43, pp. 355–376, 2001.

laboratory⁶ with these composite reactive materials, a minimal permeability k of 0.01 Darcy (10^{-14} m²) enables to avoid mass transfer limitation in the TCM reactor. As it can be noticed in Fig XXX, this permeability limit corresponds to a specific minimal porosity depending on the salt mass ratio and apparent bulk density of ENG.

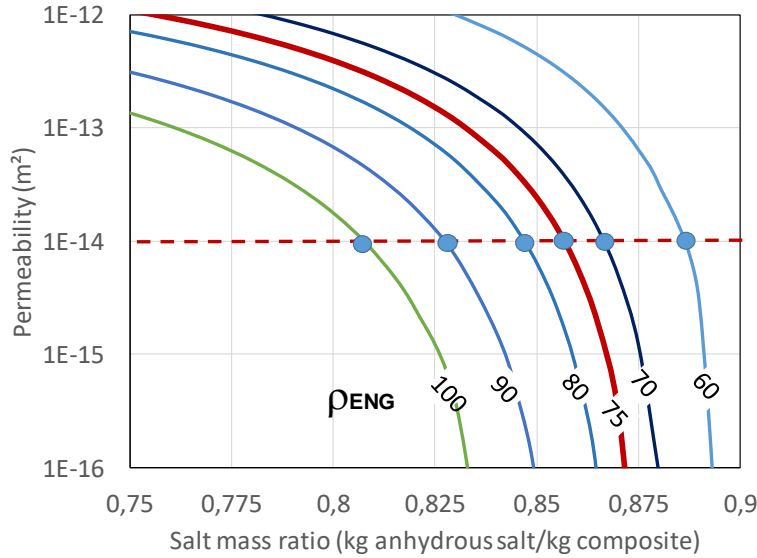


Figure 15: Evolution of permeability of the fully charged TCM material with the anhydrous salt mass ratio and the apparent bulk density of ENG

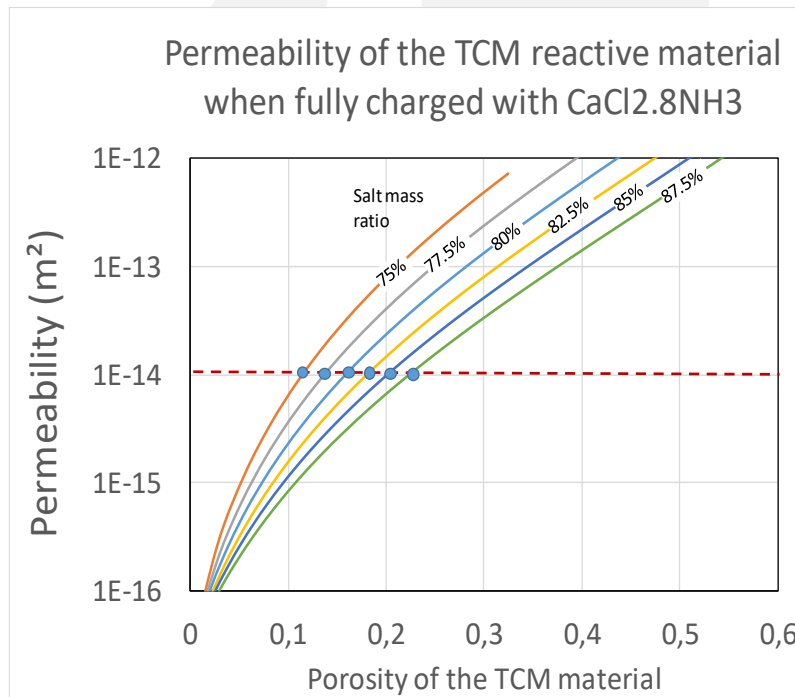


Figure 16: Evolution of NH_3 permeability of the TCM material when fully charged with $\text{CaCl}_2 \cdot 8\text{NH}_3$ as function of the porosity and anhydrous salt mass ratio.

The minimal required permeability and consequently the minimal porosity can be obtained by implementing a specific TCM material and corresponds to a pair of implementation characteristics (τ_{salt} ; ρ_{ENG}) (salt mass ratio ; apparent density of the ENG in the material), for example a TCM compound with 86.2% of salt and an apparent ENG density of 75 kg/m³.

⁶ S. Mauran, Flux de gaz en milieu poreux réactif déformable : relation entre texture, propriétés mécaniques et transferts. Incidences sur la mise en œuvre des réactifs et les performances de pompes à chaleur chimiques solide-gaz. Thèse de doctorat d'État, Université de Perpignan, France, 1990.

Of course, the decrease in the ENG apparent density of the TCM material, and also in the salt mass ratio, increases the porosity and thus the permeability, but on other hand, it also decreases the material consolidation and the heat transfer characteristics. To maintain a relatively efficient heat transfer inside the porous reactive material, a minimal thermal conductivity of 6 W/K•m must be achieved. Such condition then imposes then a minimal ENG bulk density of 75 kg/m³ in the TCM material, as the thermal conductivity is directly correlated to ENG mass into the material.

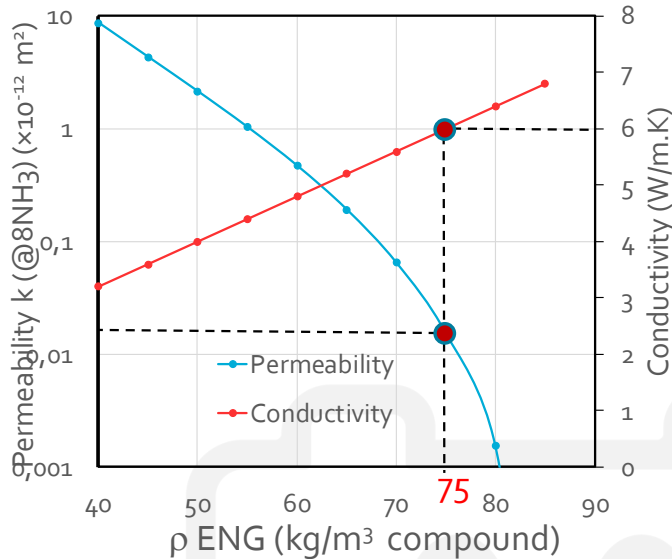


Figure 17: Evolution of the thermal conductivity and NH₃ permeability of the fully charge TCM material reactive material (CaCl₂•8NH₃)/ENG containing 85% an anhydrous salt, as a function of the apparent density of ENG in the reactive material.

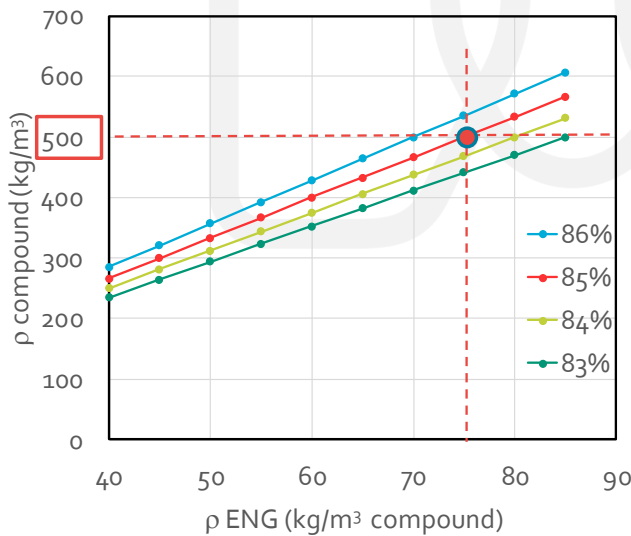


Figure 18 : Evolution the bulk density of the TCM material as a function of the apparent ENG density and the salt mass ratio.

Once the implementation parameters have been chosen in terms of composition (salt mass ratio) and consolidation degree (final bulk density, apparent ENG density), then the TCM material can be fully characterised in terms of heat and mass characteristics, porosity, energy densities considering completed reactions (only the first or the two reactions).

4.3 Final characteristics choice of the TCM material

Finally, the best implementation for the TCM material that enables a good compromise between heat transfer characteristics and mass transfer characteristics, considering the different operating constraints, should be the following:

Table 3 : TCM material characteristics

TCM material characteristics	
TCM material density	500 kg/m ³
Mass ratio and apparent density of the anhydrous salt	85 % / 425 kg/m ³
Mass ratio and apparent density of the ENG graphite	15% / 75 kg/m ³
Porosity of the TCM material @ different state of charge	
when salt is fully charged @ 2moles of NH ₃	0.621
when salt is fully charged @ 4moles of NH ₃	0.475
when salt is fully charged @ 8moles of NH ₃	0.174
Effective thermal conductivity of the TCM material	6 W/m•K
Permeability	2.4 •10 ⁻¹⁴ m ²
Max energy density obtained when $\Delta X_1 = 1$ and $\Delta X_2 = 1$	
De _{max1} (considering only 1 st reaction completed)	180 kWh/m ³
De _{max1&2} (considering both 1 st and 2 nd reaction completed)	270 kWh/m ³
Targeted TCM energy density De	200 kWh/m ³
obtained when $\Delta X_1 = 0.95$ and $\Delta X_2 = 0.32$	

The energy density of the TCM material is function of the advancements that are considered for the first and second reaction.

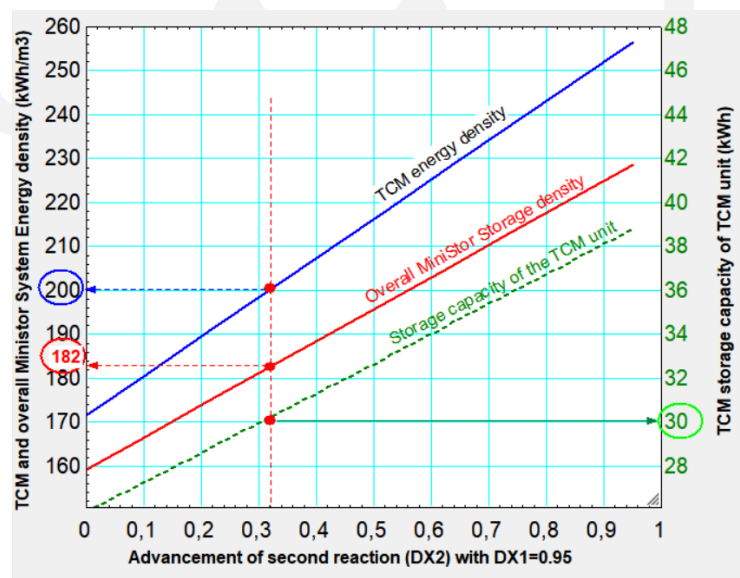


Figure 19 : Evolution of the storage energy density of the TCM material and the storage capacity of the TCM unit as a function of the advancement ΔX_2 of the second reaction considering an advancement of $\Delta X_1=0.95$ for the first reaction

Considering a realistic maximum advancement $\Delta X_1=95\%$ for the first reaction, the TCM energy density can thus evolve from 172 kWh/m³ to 256 kWh/m³ as function of the advancement ΔX_2 of the second reaction that can vary from 0 to also 95%.

The advancements of reaction ΔX_1 and ΔX_2 that are finally considered in the last line of Table 3 are dependent on the targeted energy density $De_{TCM}=200$ kWh/m³. This value has been fixed in accordance to the overall energy density that has to be reached by the whole Ministor system ($De_{glob}=182$ kW/m³ of storage material constrained by the project, i.e. 10.6 times the storage density of water) and given that the hot PCM unit provided by Sunamp should have a storage capacity of 3.6 kWh implementing a PCM material with an energy density De_{PCM} of 105 kWh/m³. Finally, the TCM unit is a very flexible storage unit as it can adapt its storage capacity by only varying the advancement of the second reaction.

For this TCM material composition according to the targeted energy density, the ammonia mass that is cycled when 1 m³ of TCM material is implemented into a reactor is defined as:

$$m_{NH3cycled} = (v_1\Delta X_1 + v_2\Delta X_2) \cdot \frac{\tau_{salt} \rho_{comp}}{Mm_{anhydrous\ Salt}} \cdot Mm_{NH3} \quad [\text{kg NH}_3/\text{m}^3 \text{ of composite}]$$

The volume and the mass of TCM reactive composite that should be required to achieve a given storage capacity Q_{stor} for the TCM reactor is then defined from the targeted energy density De of the TCM material:

$$V_{comp} = \frac{Q_{Stor}}{De} \quad \text{and} \quad M_{comp} = \rho_{comp} V_{comp}$$

The corresponding volume of reactive composite and total length of reactor tube for a given reactor diameter (here $D=114.3$ mm, ie 4"OD) are plotted on the following figure 20.

The mass of reactive salt and the corresponding cycled ammonia mass that must be implemented for a given TCM storage capacity can thus be determined by the following relations:

$$M_{salt} = \tau_{salt} \rho_{comp} V_{comp} = \tau_{salt} \rho_{comp} \frac{Q_{Stor}}{De} \quad [\text{kg of anhydrous salt}]$$

and thus

$$m_{NH3cycled} = (v_1\Delta X_1 + v_2\Delta X_2) \cdot M_{salt} \cdot \frac{Mm_{NH3}}{Mm_{CaCl2}} \quad [\text{kg NH}_3]$$

Figure 21 shows the evolutions of the mass of anhydrous CaCl₂ salt to be implemented and the corresponding mass of the cycled ammonia as a function of the energy storage by considering the targeted energy density De of 200 kWh/m³ obtained when the advancements of the reactions are $\Delta X_1 = 0.95$ and $\Delta X_2 = 0.32$. Moreover, the maximum mass of ammonia that can be cycled with the same implemented mass of salt in the TCM unit is also plotted considering the second reaction almost completed ($\Delta X_2 = 0.95$). For example, for a given TCM storage capacity of 30 kWh, the mass of TCM material CaCl₂/graphite to implement is around 75kg, the cycled ammonia is 43 kg and the maximum cyclable ammonia is 57 kg.

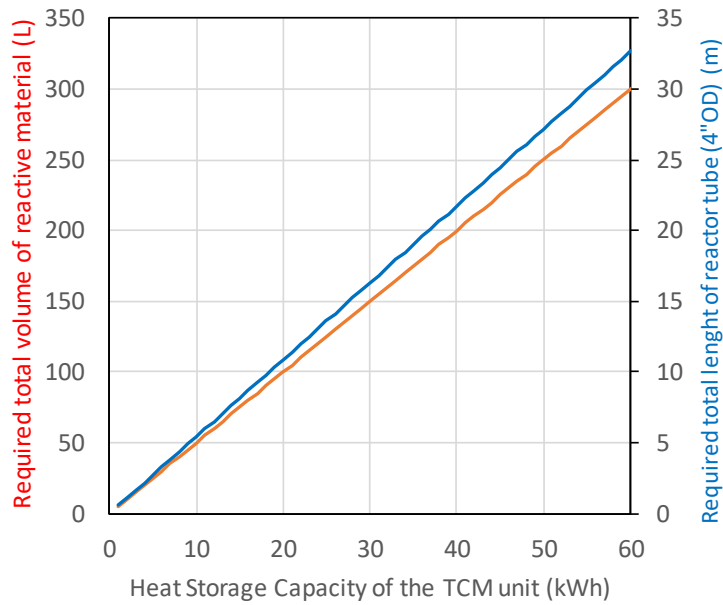


Figure 20 - Required total length of reactor tube (4"OD) as a function of heat storage capacity of the TCM unit considering advancements of reaction of reaction $\Delta X_1=0.95$ and $\Delta X_2=0.32$ to reach an energy density of 200 kWh/m^3

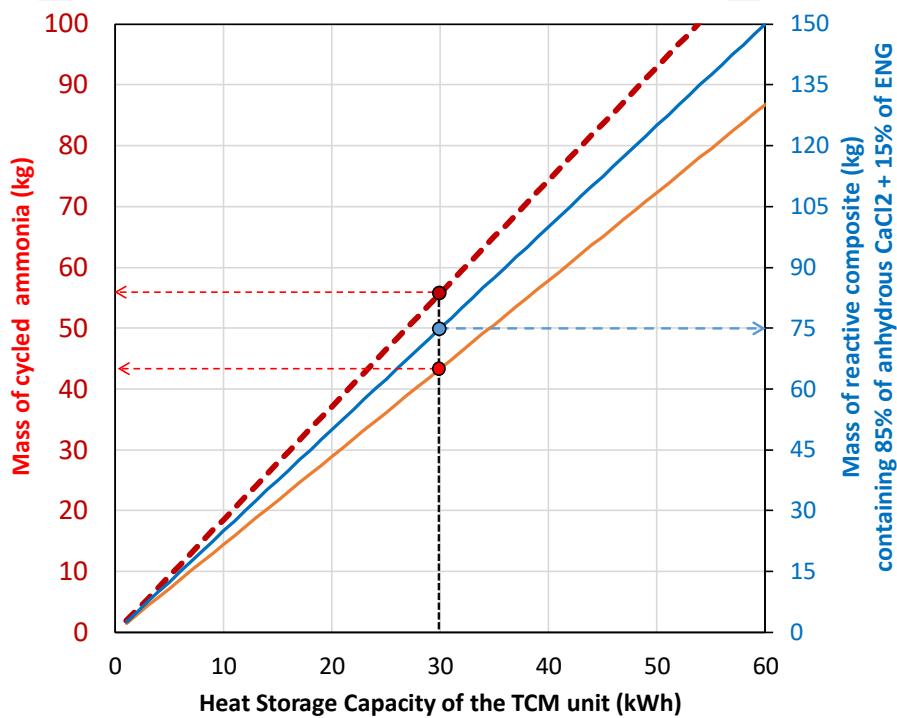


Figure 21 : Evolution of the mass of cycled ammonia (red line) and the corresponding TCM reactive material mass (blue line) to be implemented considering advancements of reaction of reaction $\Delta X_1=0.95$ and $\Delta X_2=0.32$ to reach an energy density of 200 kWh/m^3 for a given heat storage capacity of the TCM reactor. Evolution of the corresponding maximum mass of ammonia that could be cycled if the second reaction is almost completed ($\Delta X_2=0.95$).

5. Design of the TCM reactor

5.1 Model development for TCM reactor design

The dimensioning of the TCM reactor must take into account the thermal power involved. In order to assess the behaviour of the TCM reactor assisted by the NH₃ compressor during the charging phase, the following schematic frame study is defined. The dimensioning of the reactor is carried out in relation the charging phase by considering the available solar power heat source. The reactor, containing a given amount of mole of salt (N_{salt}) is heated by the solar PVT collectors. A compressor sucks the ammonia produced by the heated reactor at the pressure P_{TCM} and compress it to the condensing pressure P_{cond}. The condensation is assumed to take place at 28°C in winter (imposed by the temperature of the HP evaporator) and at 50°C in summer considering an ambient temperature of 35°C. The ammonia is then stored into a liquid reservoir at ambient temperature.

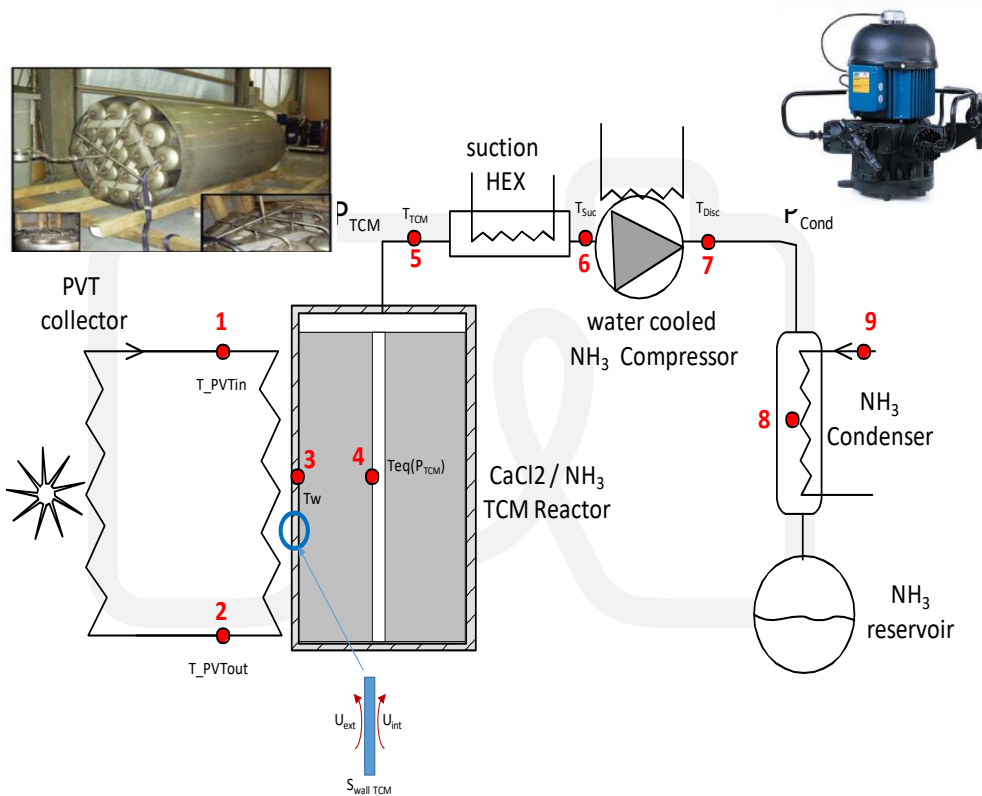


Figure 22: Schematics of the TCM unit components and the different operating variables used for the modelling of the compressor driven TCM storage during the charging phase. View of an already shell and tube type reactor experimented in CNRS lab. View of the foreseen ammonia semi-hermetic compressor (Frigopol)

The PVT collector area is designed to achieve a given maximum thermal power Q_{PVTmax} . The mass flow rate of PVT heat transfer fluid, \dot{m}_{PVT} , with a given specific heat capacity $C_{p_{PVT}}$, is chosen in such way that for this maximum thermal power the temperature difference ΔT_{PVT}^{max} of the heat transfer fluid at the inlet (T_{PVT_in}) and outlet (T_{PVT_out}) of the PVT solar field is set to 5K:

$$\dot{Q}_{PVTmax} = \dot{m}_{PVT} \cdot C_{p_{PVT}} \cdot \Delta T_{PVT}^{max}$$

Estimating a heat exchange coefficient by convection U_{W_ext} at the reactor wall (estimated to be around 200 W/m².K), this mass flow rate \dot{m}_{PVT} enables to determine the heat exchange efficiency of the reactor and thus the wall temperature T_{W_TCM} of the TCM reactor by considering it almost uniform along the reactor wall of area A_{W_TCM} :

$$\varepsilon_{HX_TCM} = \frac{T_{PVT_in} - T_{PVT_out}}{T_{PVT_in} - T_{W_TCM}} = 1 - \exp\left(-\frac{U_{W_ext} \cdot A_{W_TCM}}{\dot{m}_{PVT} \cdot C_{p_{PVT}}}\right)$$

The wall temperature (T_{W_TCM}) is of importance as it conditions the reaction rate of the reactor. The averaged reaction rate for each reaction (subscript 1 and 2 for the first and second reaction) is a function of the temperature difference between the reactor wall (T_{W_TCM}) and its equilibrium temperature T_{eq} at the pressure P_{TCM} that is imposed by the compressor.

$$\left(\frac{dX_1}{dt}\right) = \frac{\Delta X_1}{\Delta t_{react}} = \frac{U_{W_int} \cdot A_{W_TCM}}{v_1 \cdot N_{salt} \cdot \Delta H_{R1}^o} (T_{W_TCM} - T_{Eq1}(P_{TCM}))$$

$$\left(\frac{dX_2}{dt}\right) = \frac{\Delta X_2}{\Delta t_{react}} = \frac{U_{W_int} \cdot A_{W_TCM}}{v_2 \cdot N_{salt} \cdot \Delta H_{R2}^o} (T_{W_TCM} - T_{Eq2}(P_{TCM}))$$

And thus, the averaged power of the reactor can then be expressed as considering

$$\dot{Q}_{TCM} = \dot{m}_{PVT} \cdot C_{p_{PVT}} \cdot (T_{PVT_in} - T_{PVT_out}) = N_{salt} \cdot \left(v_1 \Delta H_{R1}^o \frac{\Delta X_1}{\Delta t_{react}} + v_2 \Delta H_{R2}^o \frac{\Delta X_2}{\Delta t_{react}} \right)$$

The mean mass flow rate of ammonia that the reactor produces during the decomposition when it is heated is expressed as:

$$\dot{m}_{NH3} = \left(\frac{v_1 \Delta X_1 + v_2 \Delta X_2}{\Delta t_{react}} \right) \cdot N_{salt} \cdot M m_{NH3}$$

$$\dot{m}_{NH3} = \left(\frac{U_{W_int} \cdot A_{W_TCM}}{v_1 \cdot \Delta H_{R1}^o} (T_{W_TCM} - T_{Eq1}(P_{TCM})) + \frac{U_{W_int} \cdot A_{W_TCM}}{v_2 \cdot \Delta H_{R2}^o} (T_{W_TCM} - T_{Eq2}(P_{TCM})) \right) M m_{NH3}$$

The ammonia compressor is characterized by its swept volume Q_{V_swept} (volumetric flow at nominal speed of the compressor), its volumetric efficiency η_v and its isentropic efficiency η_i . The actual volumetric flow that the compressor sucks from the TCM reactor is then expressed as:

$$Q_{V_{NH3}} = Q_{V_{swept}} \cdot \eta_v = Q_{V_{swept}} \cdot \left(1 - 0.058 \frac{P_{cond}}{P_{TCM}} \right) = \dot{m}_{NH3} \rho_{NH3_vap}(T_{suc}, P_{TCM})$$

The compressor imposes on the reactor the suction pressure P_{TCM} , and thus its equilibrium temperature. Depending on the wall temperature, the TCM reactor then produces an ammonia flow rate which must then be equal to the suction flow rate of the compressor. An iteration on the suction pressure is carried out in order to equalize these two mass flow rates: the one that can produce the reactor and the second one that is sucked by the compressor.

5.2 Design parametric study

The following graphs shows an estimation of the storage capacity that can be achieved by a TCM reactor operating during a given reaction time corresponding to the operating of the solar collectors in winter conditions. The winter conditions are relevant for the design of the TCM unit as the solar resource is lower in comparison to summer.

The parametric study is carried out by considering different specific ammonia compressors (Frigopol models 7DLY, 10DLY, 14DLY, 19DLY and 24DLY). Each of them are characterized by a specific swept volume, ie 7.22 m³/h for the 7DLY model. The results plotted on the following graphs have been obtained by keeping constant the inlet temperature of the reactor (delivered by PVT collectors) at 65°C and for an energy density of 200 kWh/m³ of TCM material.

The heat storage capacity of the TCM that can be implemented increases with the swept volumetric flow of the compressor and the reaction time. The corresponding mean thermal power, that is required for the decomposition of TCM reactor and that should be delivered by the solar collectors, evolves in a small range of variation for a given swept volume flow of the ammonia compressor.



Figure 23 - FRIGOPOL semi-hermetic Compressor

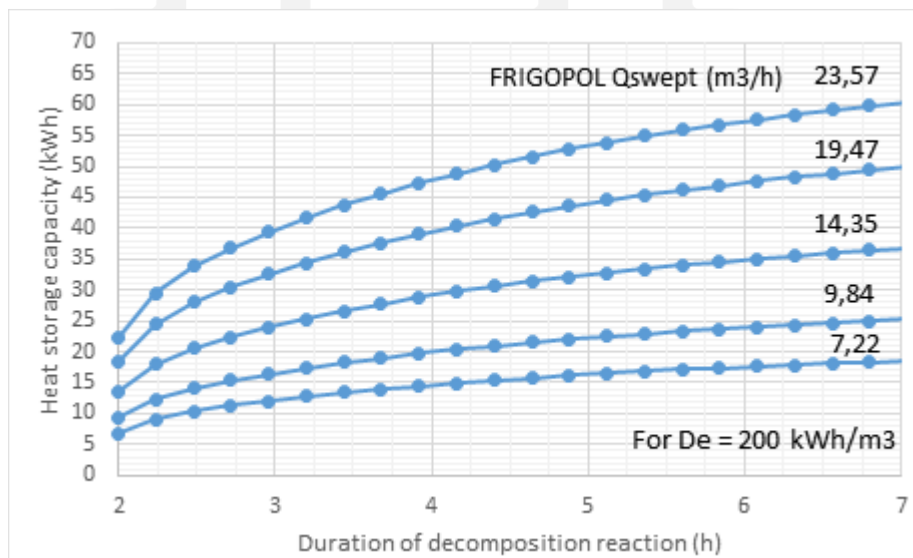


Figure 24: Evolution of the heat storage capacity of a shell and tube type TCM reactor as a function of the charging duration (i.e., solar energy collected over a given time), the maximum swept volume of ammonia compressor Frigopol models (winter conditions for inlet PVT temperature = 60°C).

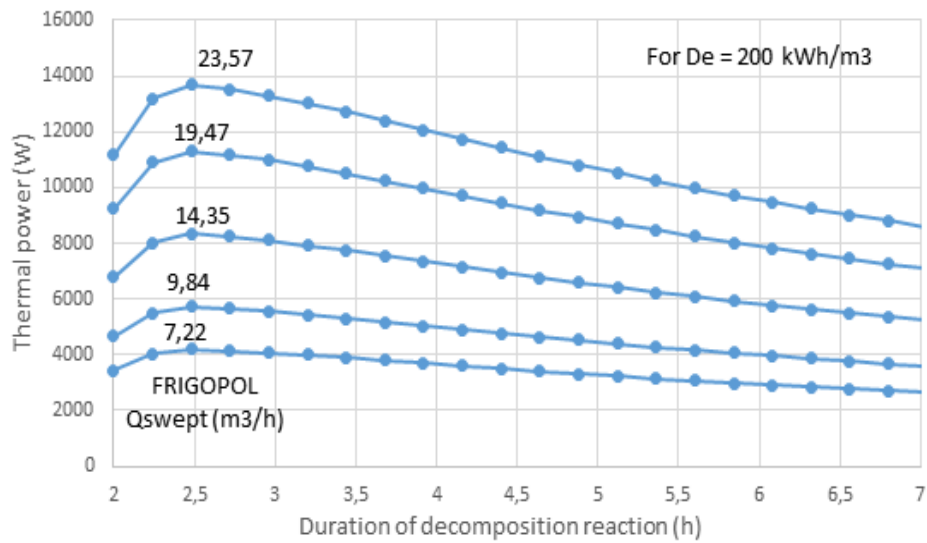


Figure 25 : Evolution of the required thermal heating power for of a shell and tube type TCM reactor, as a function of the charging duration (i.e. solar energy collected over a given time), the maximum swept volume of ammonia compressor Frigopol models (winter conditions for inlet PVT temperature = 60°C).

The following figures show the electrical power consumption of the different models of compressor and the mean volumetric flow rate that is pumped from the TCM reactor as a function of compressor's swept volume and the considered operating duration.

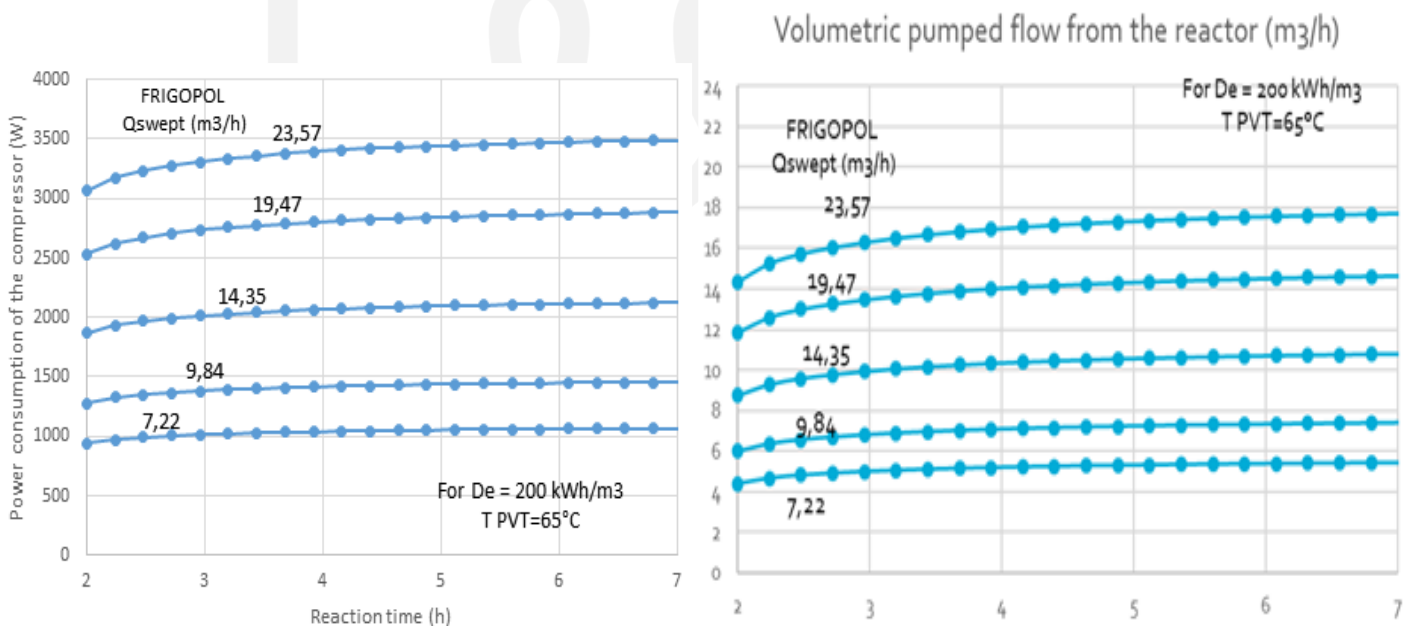


Figure 26 - Evolution of the electrical consumption of the compressor and the volumetric ammonia flow rate pumped from the reactor as function of charging phase duration

The following graphs shows an estimation of the reaction time obtained by implementing different ammonia compressors size (Frigopol models 7DLY, 10DLY, 14DLY, 19DLY) and for different storage capacity of reactor operating with variable inlet PVT temperatures and under summer or winter conditions

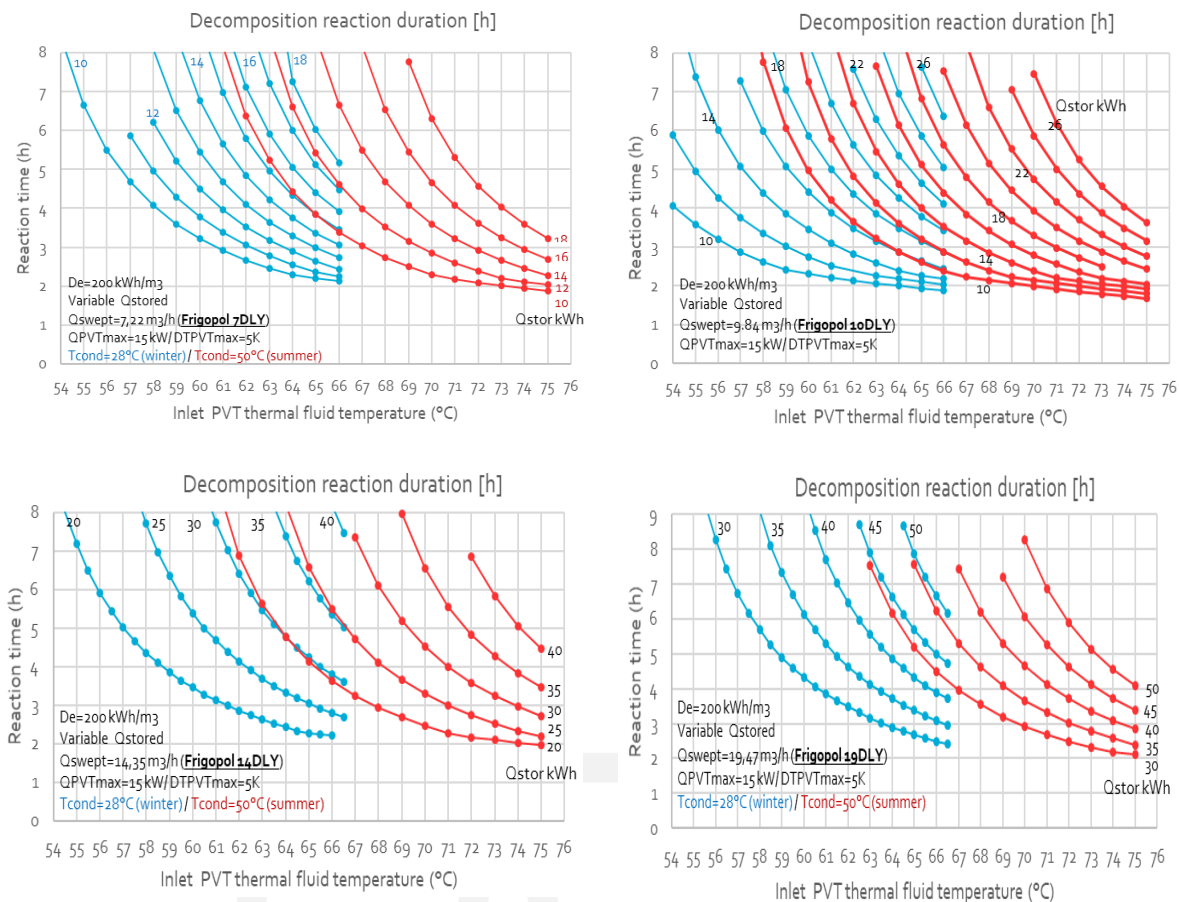


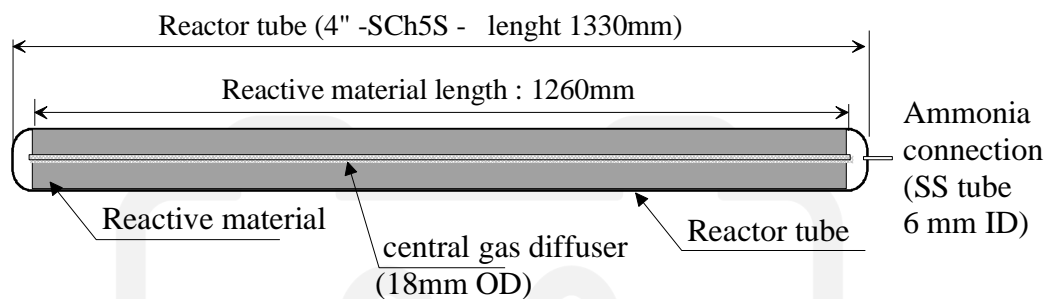
Fig 27: Simulated results of a shell and tube type TCM reactor with different storage capacities coupled to a NH₃ compressor with different given swept volumes (from 7.22 m³/h to 19.47 m³/h - Frigopol DLY models) - Required charging durations in winter (blue lines) and in summer (red lines) as a function of the inlet PVT thermal fluid temperature

This first parametric study enabled an understanding of the behaviour and performance evolution of the TCM reactor operating under different conditions and coupled to a compressor during the charging phase. This study enabled to assess which NH₃ compressor size should be chosen for a given storage capacity operating. The storage capacity of the TCM unit is limited by the available solar resource and has however to be in accordance with the energy that can be provided by the PVT solar collectors in terms of thermal power level, power duration availability and finally the temperature at which this solar energy is delivered. In this parametric study, it has been considered that the TCM reactor is heated by the solar thermal heating fluid at 65°C. If the solar heat is delivered at lower temperature, then the TCM will have to operate with a longer time to achieve a given storage capacity.

5.3 Modular design and dimensioning of the TCM reactor

It has been decided that the design of most interest and relevance to the Ministor system should be a modular design of the TCM unit. The TCM reactor of this unit is designed as a “shell and tube” type

reactor, made of a bundle of reactor tubes (4"OD schedule 5S – OD 114.3 thickness 2mm) connected together by a spider-shaped distributor. Each reactor tube is 1.33m long and contains 1.26m of reactive material composed of a recompressed mixture of 5.07 kg of anhydrous CaCl₂ and 0.90 kg of natural expanded graphite. Each reactor tube is made of **316L stainless steel, which is corrosion resistant toward the ammoniated CaCl₂ salt, which stays always in its crystalline form**. Indeed, corrosion phenomena mainly occur when the salt is solubilised in liquid ammonia or water and in the presence of oxygen. These situations never occur because the reactor tube filled with salt is first evacuated (no oxygen remains) and the solubilisation of the salt is avoided by controlling the pressure of the reactor during operation which must be kept lower than the pressure of the saturated solution (about the half that of the liquid/vapour phase change of ammonia). Furthermore, **the stainless steel grade 316L (EN 1.4435)**, is one of the most cost-effective and corrosion-resistant stainless steel. The significant presence of molybdenum (about 3%) in the 1.4435 stainless steel is well known to increase the corrosion resistance to chlorides, strong acids and bases.



Each reactor tube is filled with

- 5,97 kg of recompressed mixture (11.9 Litres) :
- 5.07 kg of anhydrous CaCl₂ + 0.90 kg of ENG

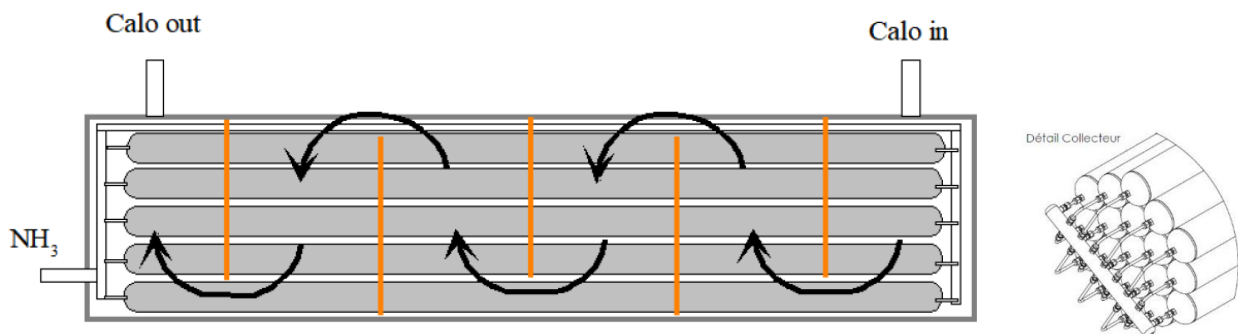


Figure 28: TCM reactor tubes characteristics and proposed shell/tube design of the TCM reactor

With such a design type, the TCM reactor storage capacity can thus be modulated by varying the number of reactor tubes that are implemented in it. Table 4 proposes two different design implementing 13 tubes leading to a 30 kWh of storage capacity and 7 tubes leading to a 16 kWh of storage capacity. **The consortium has finally considered that a storage capacity of 30 kWh is a fair compromise between the solar resource available in winter in each demo site and the corresponding heating needs.** Even if it is

oversized in winter due to the weak solar resource, in summer this storage capacity should meet the cooling needs of the building.

Table 4: Characteristics of two different design TCM storage unit for two heat storage capacity, 30 kWh with 13 reactor tubes or 16.3 kWh with 7 reactor tubes respecting the constraint of 200 kWh/m³ of TCM material

	13 tubes design	7 tubes design
TCM Heat Storage Capacity @ 60°C	30.3 kWh	16.3 kWh
Cold Storage Capacity @ 5°C	14.1 kWh	7.7 kWh
Hot PCM storage capacity unit considering a PCM energy density of 100 kW/m ³ (provided by Sunamp)	3.5 kWh	1.8 kWh
Required volume of hot PCM	35 Lit	18 Lit
Required volume of TCM material	151.1 litre	82 Litre
Mass of the TCM material (composite salt/ENG)	77.2 kg	41.7 kg
Mass of <u>anhydrous</u> CaCl ₂ salt	65.9 kg	35.5 kg
Mass of Expanded Natural Graphite (ENG)	11.3 kg	6.2 kg
Total mass of ammonia required to fully charge the TCM material from initial anhydrous salt (CaCl ₂) to the fully ammoniated salt (CaCl ₂ .8NH ₃)	78.7 kg	43.7 kg
Maximum cycled ammonia when fully discharged from CaCl ₂ .8NH ₃ to CaCl ₂ .2NH ₃ → corresponding to an energy storage capacity of 270 kWh/m ³ ($\Delta X_{1\&2} = 1$)	59.1 kg	32.0 kg
Cycled ammonia mass in normal operation to meet the targeted energy density of 200 kWh/m ³ corresponding to advancements of reaction $\Delta X_1 = 0.95$ and $\Delta X_2 = 0.32$	43.7 kg	23.7 kg
Total length of required reactive material	16.4 m	8.82
Number of reactor tubes	13 tubes	7 tubes
Length of unitary reactor tube (4"OD Sch5S)	1.33 m	1.33 m
Length of reactive material in each tube	1.26 m	1.26 m
Size of shell of the TCM storage unit (D x L)	540mm x1.45m	370mmx1.45m
Total mass of stainless steel (Shell+baffles+reactor tubes)	25+4+111=140kg	22+3+50= 75kg
Volume content of heat transfer fluid in TCM shell	122 litre	40 litre

To achieve this storage capacity (30kWh) under the specified advancements of reaction $\Delta X_1=0.95$ and $\Delta X_2=0.32$ corresponding to the nominal operating of the TCM unit to reach the targeted energy density of 200 kWh/m³, the required TCM reactive composite material is 77.2 kg, composed of 65.9 kg of anhydrous CaCl₂ salt and 11.3 kg of expanded graphite. The corresponding volume of the TCM material, considering its bulk density of 500 kg/m³, is 151.1 Litres.

However, it should be pointed out that if the solar resource is higher than expected, then more implemented ammoniated salt should be decomposed into CaCl₂.2NH₃, producing thus more ammonia gas. This results in a higher conversion rate ΔX_2 of the second reaction. In the extreme case that all of the implemented salt is decomposed into CaCl₂.2NH₃, the total amount of ammonia that is produced should be 59.1 kg. In this case, the TCM unit stores more energy (around 39 kWh) and its achieved energy density is higher (256 kWh/m³). Moreover, it should also be pointed out that during the first

commissioning phase, the initial state of the salt is in anhydrous form (CaCl_2). In order to put in operation the TCM unit, the salt has then to be first fully ammoniated into $\text{CaCl}_2 \cdot 8\text{NH}_3$, and the required ammonia to fully ammoniate the 65.9 kg of anhydrous salt is 78.7 kg of ammonia.

The TCM reactor will thus be composed of 13 reactor tubes that are placed into a shell where the solar heat transfer fluid (HTF) circulates perpendicularly to the reactor tube thanks to baffles spaced about 30cm apart. The reactor tubes are spaced 5mm apart for enabling the correct circulation of the HTF and ensuring an efficient thermal exchange. In this way, the shell should have a diameter of 540mm and a total length of approximately 1.45m. The water content of the TCM unit should be 120 litres. The total mass of this 30 kWh TCM storage unit should be around 420 kg when fully loaded with HTF and ammonia. By connecting 3 or 4 reactor tubes together, this design enables to modulate and adapt the storage capacity to the solar heat source which is variable. In this way, the storage capacity of the TCM reactor can be modulated from 7 to 30 kWh by adapting the number of reactors that are connected.

All reactor tubes are connected together at one end by a spider-shaped distributor, allowing the correct flow of the ammonia gas from each reactor tube in desorption phase (storage mode) or to each reactor tube in absorption phase (heat/cold production mode). The flow from/to each reactor tube is achieved independently and as needed to equalize the pressure in all reactor tubes. In fact, each reactor tube when heated (storage mode) or cooled (production phase) produces or absorbs ammonia independently and according to its needs resulting from the thermal equilibrium deviation that is imposed on it. Such a spider-shaped distributor is therefore the most appropriate means of connecting and ensuring the proper flow of ammonia from/to each reactor tube that constitutes an independent source or sink of ammonia.

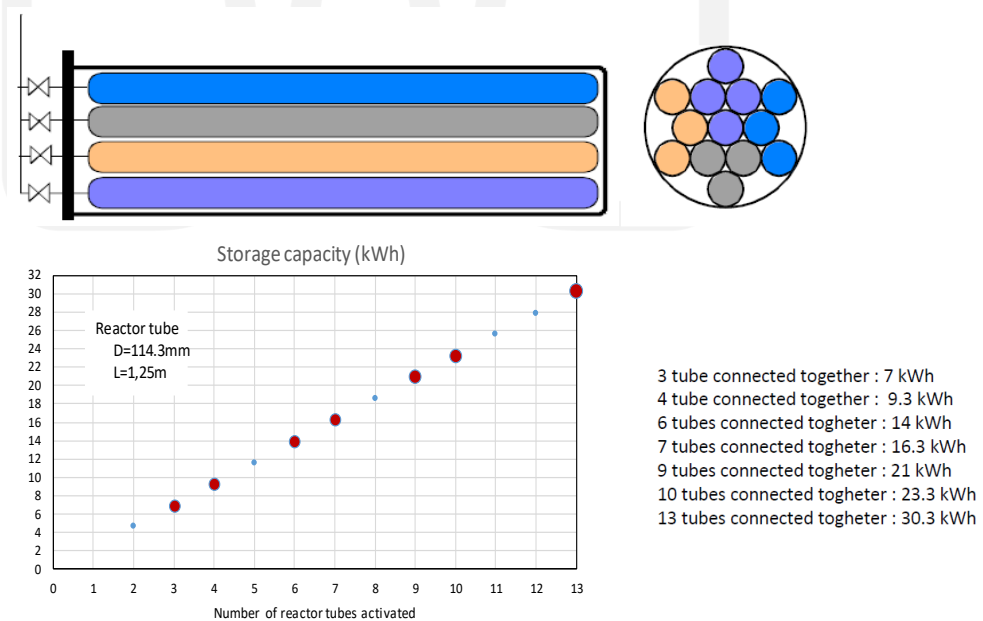


Figure 29: TCM design solution for more energy flexibility. The bundle of reactor tubes can be arranged in sub-set of 3 or 4 reactor tubes in order to modulate the energy capacity of the reactor. Evolution of the TCM storage capacity for a given number of connected reactor tubes

For the different storage capacities (or number of connected tubes), the simulated results that are presented below have been carried out considering the operating conditions summarized in the following table. From these conditions, several criterion and operating parameters have been calculated such as

the required operating duration, the resulting operating conditions of the compressor, the TCM operating temperatures, etc.

Table 5 : Operating parameters of the TCM storage for winter and summer conditions

TCM storage operating parameters	Winter conditions	Summer conditions
Storage capacity	30 kWh of heat	15 kWh of cold
Inlet thermal power (Solar collector)	variable from 500 to 5000W	
Inlet TCM reactor temperature	60°C	75°C
Temperature difference TCM thermal fluid	5 K	5 K
Evaporating temperature and pressure	-5°C	6°C
Condensing temperature and pressure	28°C (11 bars)	50°C (20.3 bars)
Outside ambient temperature	0°C	35°C
Hot PCM temperature	58°C	n/a
Cold PCM temperature	n/a	11°C

The following graphs shows the impact of the thermal power provided by the solar field collector in terms of required operating duration to achieve the targeted energy density of the TCM unit (200 kWh/m³), required heat transfer fluid flow rate, the electrical consumption of the compressor, the thermal power of condenser, etc.

In order to maintain the temperature difference of 5K of the thermal fluid between the inlet and the outlet of the TCM reactor, the flow rate of the heat transfer fluid must evolve with the thermal power as depicted on the beside graph.

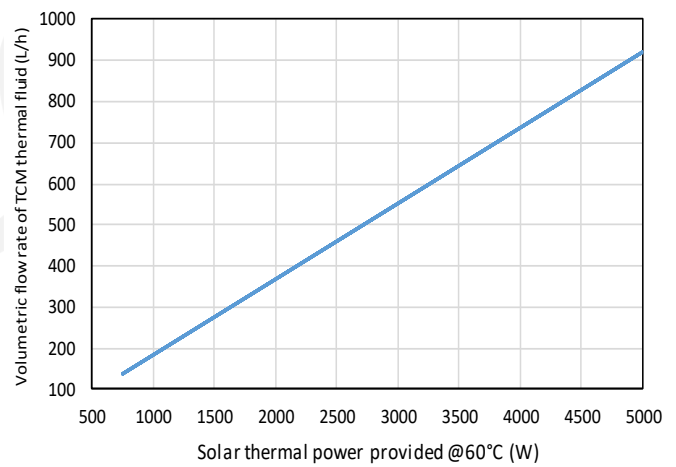


Figure 30: Volumetric flow of the Solar heat transfer fluid as a function of the thermal power

The operating duration that is required for reaching the targeted energy density of 200 kW/m³ depends on the considered storage capacity (i.e.: the number of reactor tube that are connected) and the thermal power that can be provided by the solar collectors. This duration has to correspond to the operating time of the solar thermal fluid loop providing the required heat at the minimum temperature of 60/55 °C in winter (or 75/70°C in summer) for charging of the TCM reactor. The charging phase may be carried out in 1 day, 2 days or 3 days depending on the solar resource availability. The coupling of several sets of reactor tubes can offer the possibility to exploit low solar resource over 1,2 or 3 days.

The beside graph shows that the wall temperature of the reactor decreases with the thermal power. In fact, as the heat transfer surface of the reactor is fixed by the implemented reactor tubes size, the mean temperature difference between the heating fluid and the wall of the reactor must increase with the exchanged thermal power.

Consequently, the decrease of the wall temperature impacts also the operating pressure of the reactor that also decreases.

If this pressure drops below a critical value for the compressor, then the compressor will stop because the compression ratio will be higher than the maximal achievable value by the compressor (approx. 6 to 7)

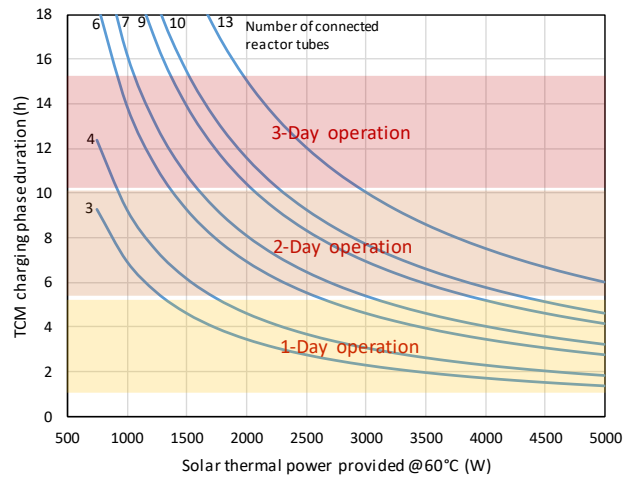


Figure 31: Evolution of the operating duration for a full charging of the 30kWh TCM reactor as a function of the thermal power provided by the solar field

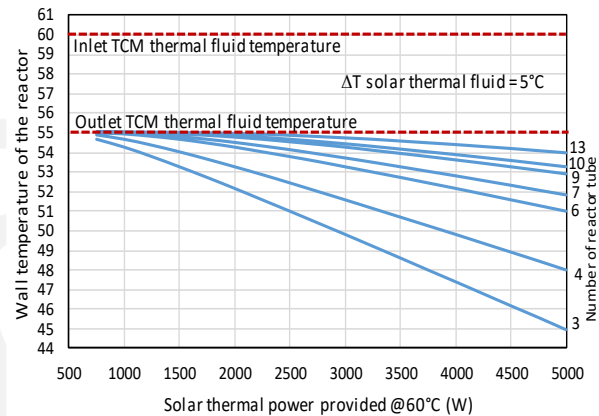


Figure 32: Evolution of the wall temperature of the 30kWh TCM reactor as a function of the solar thermal power provided at 60°C

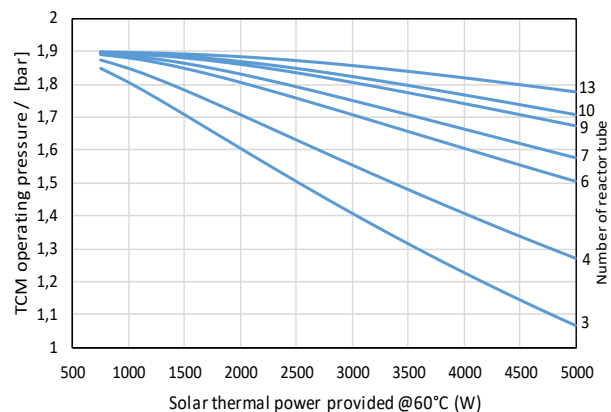


Figure 33: Evolution of the operating pressure of the TCM reactor as a function of the solar thermal power provided at 60°C

The electrical consumption of the compressor increases with the solar thermal power and for decreasing number of reactor tubes that are connected. For a solar thermal of 2500 W, the electrical power that is consumed by the compressor is around 500 to 700 W.

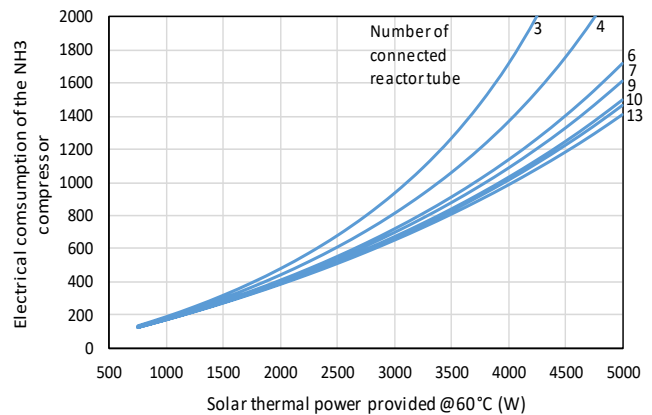


Figure 34: Evolution of the electrical consumption of the TCM reactor as a function of the solar thermal power provided at 60°C

The graph on the side shows how the required swept volume flow rate of the compressor evolves as a function of the TCM thermal power. The required swept volume increases with the TCM heating thermal power provided by the solar loop. Consequently, this evolution shows that it is necessary to control and adapt the rotation speed of the compressor to the heating power supplied to the TCM reactor. As it can be noticed, for a thermal power of 2500 W the required swept volume varies between 35 to 55%. This means that the smallest Frigopol compressor model is still oversized for the Ministor application

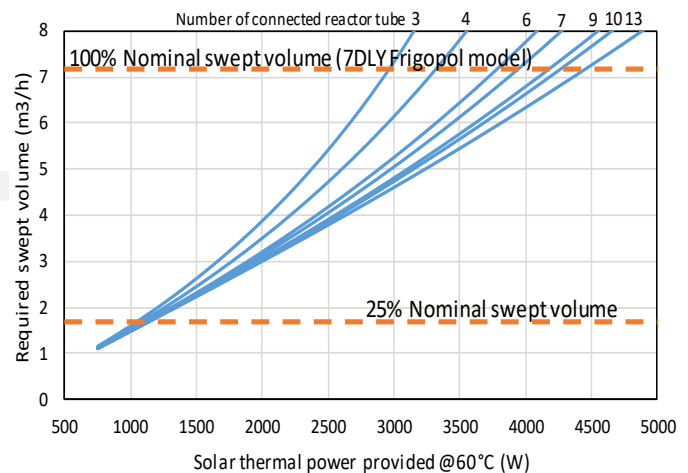


Figure 35: Evolution of the swept volume to be applied to the Frigopol 7DLY compressor model

The beside graph shows how evolves the thermal power of the condenser, for which the condensing temperature is set at 28°C by the propane heat pump. For a solar thermal power of 2500W, the power of the condenser is relatively stable at approximately 1500 -1700 W.

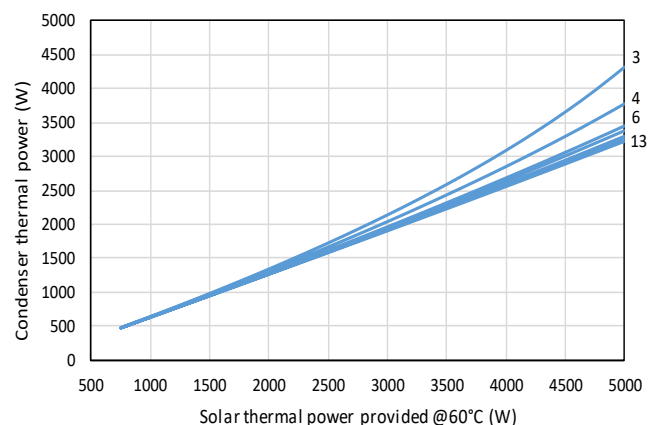


Figure 36: Evolution of the condenser thermal power operating at 28°C

6. Conclusions

This deliverable discusses and summarises the work done to define the appropriate TCM reactive material that should be implemented as well as the design of the TCM reactor developed in the framework of the Ministor project. The TCM reactive material consist of a recompressed mixture of calcium chloride and expanded natural graphite, which globally improves the heat and mass transfer characteristics compared to a reactive material consisting of salt alone.

Firstly, criteria for choosing the best implementation (mass composition of the salt/graphite mixture, degree of compression / consolidation) of this TCM material have been detailed. Based on the CNRS-PROMES knowledge of such material, a reactive material is then proposed by considering the minimum thermal conductivity ($5 \text{ W/m}^2\cdot\text{K}$) and gas permeability (10^{-14} m^2) that the material should have to avoid heat and mass transfer limitations inside. This study has led to consider a TCM reactive material composed of 85% anhydrous calcium chloride mixed expanded natural graphite (15%), such a mixture is then compressed to obtain a consolidated material with a bulk density of 500 kg/m^3 .

Secondly, a steady state model has been developed to propose a design of the TCM reactor in which the consolidated material is placed. This model has enabled to carry out a parametric study for a better understanding of the behaviour of the coupling TCM reactor with the ammonia compressor during the charging phase. It results from this study that the size of the TCM reactor must be in accordance with the solar resource in term of a minimal thermal power available a minimum required temperature over a given duration. It helped also to define the requirements of the compressor definition in term of swept volume flow and showed how this swept volume should be adapted to the provided solar thermal power by controlling its rotation speed.

Finally, in agreement with the consortium, it has been decided to consider a 30 kWh storage capacity for the TCM unit, in accordance with the availability of the solar resource on each demo sites. A design of TCM reactor was then proposed based on conventional "shell and tubes " heat exchangers design. It consists of a bundle of a 13 reactor tubes (stainless steel 316L, diameter 4"OD Sch5S, useful reactive material length 1260mm with a central gas diffuser of 18mm diameter), which are arranged in sets of 3 or 4 reactor tubes to provide more flexibility in the operating of the TCM unit regarding the solar resource availability. All the 13 reactor tubes are placed in a shell and held by 4 equally spaced baffles to make the heat transfer fluid circulate perpendicularly to the reactor tubes. This configuration increases the heat transfer coefficient at wall of the reactor tubes.

The resulting TCM reactor has then the same design for all demo sites. However, for some demo sites such as the one located in Cork, although the TCM unit may be oversized in relation to the capacity of solar field to provide the appropriate thermal power, an auxiliary heating system should be foreseen and installed to allow for full charging of the reactor during weak solar irradiation days in winter. This back-up system should increase the flexibility of use of the TCM storage unit.

7. References

- Clean energy for all Europeans package. https://ec.europa.eu/energy/topics/energy-strategy/clean-energy-all-europeans_en: European Commission; Published: 20 October 2017
- C. Coste, S. Mauran, G. Crozat. Procédé de mise en oeuvre de reaction gaz-solide. US Patent 4595774 (Juin 1983)
- Ferrucci F, Stitou D, Ortega P, Lucas F. Mechanical compressor-driven thermochemical storage for cooling applications in tropical insular regions. *Applied Energy*. 2018;219:240-55.
- Driss Stitou, Nathalie Mazet, Sylvain Mauran, Experimental investigation of a solid/gas thermochemical storage process for solar air-conditioning, *Energy*, Volume 41, Issue 1, May 2012, Pages 261-270, ISSN 0360-5442, <http://dx.doi.org/10.1016/j.energy.2011.07.029>.
- Oliveira RG, Wang RZ, Wang C. Evaluation of the cooling performance of a consolidated expanded graphite-calcium chloride reactive bed for chemisorption icemaker. *International Journal of Refrigeration*. 2007;30:103-12.
- Oliveira RG, Wang RZ. A consolidated calcium chloride-expanded graphite compound for use in sorption refrigeration systems. *Carbon*. 2007;45:390-6.
- Driss Stitou. Transformation, Conversion, Stockage, Transport de l'énergie thermique par procédés thermochimiques et thermo-hydrauliques. HDR Thesis. Université de Perpignan, 2013.
- Mauran S, Lahmidi H, Goetz V. Solar heating and cooling by a thermochemical process. First experiments of a prototype storing 60kWh by a solid/gas reaction. *Solar Energy*. 2008;82:623-36.
- Hüttig G.F., Martin W., Über die Ammoniakate des Baryumhalogenide, *Zeitung Anorganische und Allgemeine Chemie*, 125, 269-280, 1922
- Sakamoto Y, Yamamoto H. Performance of Thermal Energy Storage Unit Using Solid Ammoniated Salt (CaCl₂-NH₃ System). *Natural Resources*. 2014;5:337-42.
- Zhang Y, Wang R. Sorption thermal energy storage: Concept, process, applications and perspectives. *Energy Storage Materials*. 2020;27:352-69.
- Van der Pal M, Critoph RE. Performance of CaCl₂-reactor for application in ammonia-salt based thermal transformers. *Applied Thermal Engineering*. 2017;126:518-24.
- Neveu P. Development of a numerical sizing tool for a solid-gas thermochemical transformer - I. Impact of the microscopic process on the dynamic behaviour of a solid-gas reactor, *Applied Thermal Engineering*, 1997, 17 (6), 501-518
- Fitó J, Coronas A, Mauran S, Mazet N, Perier-Muzet M, Stitou D. Hybrid system combining mechanical compression and thermochemical storage of ammonia vapor for cold production. *Energy Conversion and Management*. 2019;180:709-23.
- Goetz V., Spinner B., Lepinasse E., A solid-gas thermochemical cooling system using BaCl₂ and NiCl₂, *Energy*, 22 (1), 49-58, 1997.